Dissertationes Forestales 179

Boreal forest albedo and its spatial and temporal variation

Nea Kuusinen

Department of Forest Sciences
Faculty of Agriculture and Forestry
University of Helsinki

Academic dissertation

To be presented, with the permission of the Faculty of Agriculture and Forestry of the University of Helsinki, for public criticism in room 10, Main building (Fabianinkatu 33, Helsinki), on November 7th 2014, at 12 o'clock noon.

Title of dissertation: Boreal forest albedo and its spatial and temporal variation

Author: Nea Kuusinen

Dissertationes Forestales 179

http://dx.doi.org/10.14214/df.179

Thesis supervisors:
Dr. Frank Berninger
Department of Forest Sciences, University of Helsinki, Finland
Prof. Pauline Stenberg
Department of Forest Sciences, University of Helsinki, Finland
Prof. Eero Nikinmaa
Department of Forest Sciences, University of Helsinki, Finland
Dr. Albert Porcar-Castell
Department of Forest Sciences, University of Helsinki, Finland

Pre-examiners:
Prof. Tiit Nilson
Tartu Observatory, Estonia
Dr. Alessandro Cescatti
European Commission, Joint Research Centre, Ispra, Italy

Opponent:
Dr. Pierre Bernier
Canadian Forest Service, Natural Resources Canada, Québec, Canada

ISSN 2323-9220 (print)
ISBN 978-951-651-447-8 (paperback)
ISSN 1795-7389 (online)
ISBN 978-951-651-448-5 (pdf)

2014

Publishers:
Finnish Society of Forest Science
Finnish Forest Research Institute
Faculty of Agriculture and Forestry at the University of Helsinki
School of Forest Sciences at the University of Eastern Finland

Editorial Office:
The Finnish Society of Forest Science
P.O. Box 18, FI-01301 Vantaa, Finland
http://www.metla.fi/dissertationes

Kuusinen, N. 2014. Boreal forest albedo and its spatial and temporal variation.
Dissertationes Forestales 179, 48 p.
http://dx.doi.org/10.14214/df.179

Surface albedo refers to the fraction of shortwave solar irradiance that is reflected by a surface. Accurate characterisation of the albedo of various land cover types is required for evaluating the energy exchange between the Earth's surface and the atmosphere. The optical and structural properties of a surface determine its albedo. Boreal forest albedo can vary due to factors such as tree species composition, forest structure, understorey vegetation composition, and seasonal changes in vegetation and snow cover.

The aim of this study was to characterise typical albedos of Finnish forests dominated by different tree species, evaluate the seasonal variation in forest albedo, and to estimate the effects of structural forest variables and understorey composition on forest albedo or spectral reflectance. To achieve these aims, forest albedo was measured in-situ using pyranometers, estimated from satellite data and calculated using a forest albedo model. Unmixing methods were used to estimate forest albedo from coarse spatial resolution MODIS albedo retrievals and understorey spectral reflectance from Landsat observations.

Mature or middle aged pine, spruce and broadleaved deciduous (mainly birch) forests had distinctly different albedos in both summer and winter. Coniferous forest albedo was lower and showed less seasonal variation than albedo in open areas or broadleaved deciduous forests. Albedo of pine was somewhat higher than that of spruce. Snow cover on the ground and canopy increased forest albedo. Young stands with an assumedly high proportion of deciduous species in the under- and overstorey were characterised by a higher albedo than the mature coniferous forests. The high albedo at early succession rapidly decreased as the forest matured. The forest floor was typically covered by green understorey vegetation with rather low albedo, which decreased the influence of a changing canopy cover or leaf area index (LAI) on forest albedo. The spectral reflectances of the understorey varied with site fertility and forest age.

Keywords: forest reflectance, remote sensing, seasonality, canopy snow interception, unmixing

ACKNOWLEDGEMENTS

First I want to thank my supervisors Frank Berninger, Albert Porcar-Castell, Pauline Stenberg and Eero Nikinmaa. Any of this work would not have been possible without your knowledge, patience and ideas. You were always confident about the work and found time to teach me how to do research and encouraged me to think and develop new ideas. Special thanks belong to my unofficial supervisor Erkki Tomppo, who was willing to spend so much time on this work and let me do the final corrections for the thesis during my working hours in Metla.

I am in a great debt to the technicians at Hyytiälä. Janne Levula, Erkki Siivola, Reijo Pilkottu, Heikki Laakso and others were more patient than I deserved and made the albedo measurements possible. Also thanks to the summer workers who helped in moving the mast. Many thanks to Caroline Nichol, who took me to Edinburgh in the midst of the busiest Christmas season. My co-authors Pasi Kolari, Petr Lukeš and Yanmin Shuai were of valuable help, thank you. I also want to thank my pre-examiners Tiit Nilson and Alessandro Cescatti as well as the reviewers of the articles.

The study was funded by the Helsinki University Center for Environment (HENVI), EU FP7 Infrastructure project ExpeER, and the Center of Excellence in Physics, Chemistry, Biology and Meteorology of Atmospheric Composition and Climate Change of the Academy of Finland.

LIST OF ORIGINAL PUBLICATIONS

This thesis is based on the following research articles, which are referred to in the text by their Roman numerals. Articles I-IV are reprinted with the permission of publishers. Article V is the authors' version of the submitted manuscript.

I Kuusinen N., Kolari P., Levula J., Porcar-Castell A., Stenberg P., Berninger F. (2012). Seasonal variation in boreal pine forest albedo and effects of canopy snow on forest reflectance. Agricultural and Forest Meteorology 164: 53-60. http://dx.doi.org/10.1016/j.agrformet.2012.05.009

II Kuusinen N., Lukeš P., Stenberg P., Levula J., Nikinmaa E., Berninger F. (2014). Measured and modelled albedos of Finnish boreal forest stands of different species, structure and understory. Ecological Modelling 284: 10-18. http://dx.doi.org/10.1016/j.ecolmodel.2014.04.007

III Kuusinen N., Tomppo E., Berninger F. (2013). Linear unmixing of MODIS albedo composites to infer subpixel land cover type albedos. International Journal of Applied Earth Observations and Geoinformation 23: 324-333. http://dx.doi.org/10.1016/j.jag.2012.10.005

IV Kuusinen N., Tomppo E., Shuai Y., Berninger F. (2014). Effects of forest age on albedo in boreal forests estimated from MODIS and Landsat albedo retrievals. Remote Sensing of Environment 145: 145-153. http://dx.doi.org/10.1016/j.rse.2014.02.005

V Kuusinen N., Stenberg P., Tomppo E., Berninger F. Variation in understory and canopy reflectance during stand development in Finnish coniferous forests. Manuscript.

Nea Kuusinen was the main author of all the articles. She collected the field material of study II with the help of the technicians from the Hyytiälä research station. The measurements used in study I were collected as part of the permanent measurements of the Hyytiälä research station. Kuusinen analysed all the data used in the studies except for the Landsat albedos in study IV, which were kindly computed by Dr. Yanmin Shuai. All authors participated in discussing the studies and commenting on the manuscripts.

TABLE OF CONTENTS

1 INTRODUCTION

1.1 Background

Albedo is defined as the fraction of incident shortwave radiation that is reflected by a surface. Integrated over the whole spectrum of solar irradiance, albedo determines the shortwave part of the net radiation, and is thus a key variable in meteorological studies and climate predictions (Dickinson 1983; Sellers et al. 1995). Optical properties and surface roughness, as well as the angular and spectral distribution of incident radiation affect albedo. Field measurements of albedo go back to the early 1900s (e.g. Ångtröm 1925; Monteith 1959), when most measurements were conducted on short vegetation or bare soil. Not much later, albedo measurements were included in studies evaluating the energy balance of forest stands (Federer 1968; Tajchman 1972; Moore 1976; McCaughey 1981). Extensive research on the albedo of different natural surfaces was also conducted in the territory of the former Soviet Union (see Kondratyev 1969). Methods for estimating surface albedo from multidirectional observations of spaceborne instruments have been developed during the past few decades. These albedo estimates provide an efficient means to monitor changes in global albedo, but can also be useful when the interest is in local-scale albedo dynamics. Local environmental conditions and land use patterns can cause seasonal and periodic variation in albedo. For example, a strong seasonal variation in albedo is distinct to the boreal zone with snowy winters, and rotation forestry with periodic clear-cut harvesting can induce both abrupt and gradual changes in forest albedo. Quantification of surface albedo variation under different management and environmental conditions may help to evaluate the total impact of land use and silvicultural practices as well as that induced by changing climatic conditions on the local radiant energy balance.

1.2 Boreal forests and climate

Boreal forests expand over the vast land areas of European and Asian Russia, Canada and Fennoscandia, constituting circa one third (13.7 million km^2) of the Earth's forested area (Grace 2004). Boreal forests are characterised by extreme temperature variations and pronounced seasonality with long, snowy winters and short growing seasons. The harsh environmental conditions driven by low solar irradiance create boundaries for energy and mass transfer between northern forests and the atmosphere. On the other hand, boreal forests influence their locate climate by e.g. absorbing more solar radiation than the tundra ecosystem bordering the boreal forest in the north (Larsen 1980). It has thus been suggested that the geographic distribution of boreal forests in the north affects the position of the polar front and thus the location of the tundra-taiga boundary (Bonan et al. 1992; Pielke and Vidale 1995).

The exchange of matter and energy between forests and the atmosphere is sometimes divided into biogeochemical and -physical interactions. The first concept refers to the absorption or release of chemical compounds, such as carbon dioxide (CO_2), nitrogen compounds, methane (CH_4) or biogenic volatile organic compounds by the ecosystem. Trees bind atmospheric CO_2 to their living biomass during growth, which reduces the absorption of terrestrial longwave radiation in the atmosphere and has a cooling influence on the climate. Carbon accumulation in vegetation is relatively slow in the boreal

environment, and a large part of the carbon in boreal forests can be found in soils (Alekseyev and Birdsey 1998). The biogeophysical effects refer to the exchange of energy between the surface and the atmosphere. The net radiative energy balance (R_n) of a surface is determined as the sum of the net shortwave (R_{ns}) and net longwave (R_{nl}) radiation, where R_{ns} is the difference between incoming shortwave solar radiation (0.2–5 μm) and outgoing (reflected) shortwave radiation from the Earth's surface, and R_{nl} is the difference between the longwave radiation (5–100 μm) emitted in the atmosphere and reaching the ground and that emitted by the surface. R_n is partitioned into sensible and latent heat fluxes, ground heat flux and a small part is bound by photosynthesising plants to form carbon compounds. Due to the often lower surface albedo and emission of longwave radiation, forests are typically characterised by a higher net radiation than open, short vegetation types (McCaughey 1981; Rouse 1984; Sharratt 1998; Betts et al. 2007; Teuling et al. 2010). Aerodynamically rough forest canopies enhance the turbulent transport of sensible heat, which decreases the surface temperature and therefore the longwave emission from forests compared to that of open vegetation during the snow-free time. Coniferous boreal forests are reported to have a relatively high sensible heat flux density because of the above mentioned factors, while the low transpiration level may reduce the latent heat flux of conifers compared to deciduous broadleaved trees or some well-drained open vegetation types (Lafleur and Rouse 1995; Baldocchi et al. 2000; Eugster et al. 2000; Betts et al. 2007). A high ratio of sensible to latent heat flux (Bowen ratio) may increase the depth of the boundary layer and decrease cloud cover, thus increasing the surface net radiation by allowing more solar radiation to enter the surface (Betts et al. 2007). The deep boundary layer and entrainment of dry air can additionally influence evaporation and transpiration from vegetation (Baldocchi et al. 2000). On the other hand, high evapotranspiration might increase the atmospheric water vapour content and thus increase the absorption of terrestrial longwave radiation.

Boreal coniferous forests are characterised by a lower albedo than open vegetation, particularly in winter when the snow-covered ground is shadowed by trees (Betts and Ball 1997; Sharratt 1998; Moody et al. 2007). Several studies have consequently found that a replacement of boreal forests with bare ground or open vegetation would lead to a locally or regionally cooling climate (Otterman et al. 1984; Thomas and Rowntree 1992; Bonan et al. 1995). When this albedo-induced cooling is paralleled to decreased carbon sequestration and changes in evapotranspiration, the deforestation/afforestation in the boreal zone is still concluded to lead to global cooling/warming (Betts 2000; Bala et al. 2007; Bathiany et al. 2010). In contrast, Arora and Montenegro (2011) concluded that afforestation of 50% of the croplands in the boreal zone would lead to a slight cooling at the global scale. Such studies enlighten the magnitude and proportions of the carbon- and albedo-related interactions of boreal forests with the climate, but the deforestation of large areas is hardly prudent in reality. The question of whether climatic benefits could be achieved by optimising forest management chains to consider the effects of both carbon sequestration and albedo, and possibly also other biogeochemical and -physical effects, has only recently been raised (Anderson et al. 2010). Some results have, however, already been gained: Thompson et al. (2009) studied the optimal rotation length of Canadian forests when carbon- and albedo-related radiative forcing was considered in forest management decision-making. They found that optimal rotation length was shorter if both albedo- and carbon-related effects are considered, compared to the scenario where only carbon was taken into account. Bright et al. (2014) suggested that favouring deciduous broadleaved species instead of evergreen conifers in Norway would lead to direct cooling at the global scale.

Betts (2007) pointed out that global-scale climate predictions or impact studies often neglect important processes or feedbacks, such as the impact of increasing atmospheric CO_2 concentration on plant transpiration or growth, the increase in soil respiration due to warmer temperatures, the change in local hydrology and convective heat partitioning due to land cover change and boreal forest expansion to the north. Davin et al. (2007) obtained results implying that the global temperature response to a change in surface albedo and evapotranspiration following anthropogenic land conversion is not equivalent to a radiatively equivalent change in CO_2 concentration, and thus questioned the use of radiative forcing units when estimating the climatic effects of land use change. It has moreover been noted that boreal forests can increase cloud albedo through biogenic volatile organic compound emissions, and thus cause a reduction in radiative forcing compared to short arctic vegetation (Spracklen et al. 2008). Yet, a special uncertainty related to boreal zone climate modelling is that of snow albedo. The land surface models used in the weather and climate forecasting models feature different snow albedo parameterisations, all of which do not explicitly take into account the effect of forest canopy on the snow-covered surface albedo (Qu and Hall 2007; Wang and Zeng 2010). Variation in snow albedo parameterisations then results in significant differences in the predicted snow albedo feedback (Qu and Hall 2007). Snow albedo feedback refers to a situation, where the warming climate reduces the extent of snow cover, and the following decrease in albedo further enhances the warming.

1.3 Forest reflectance and albedo

The albedo of a surface refers to the fraction on incident solar radiation that is reflected by the surface to the entire upper hemisphere, and can thus be derived as an integral of the directional reflectances over the upper hemisphere. A quantity that would be derived if the surface was hypothetically illuminated from a single direction only, i.e. from a point source, is called directional-hemispherical reflectance (DHR), or black-sky albedo (Schaepman-Strub et al. 2006). In ambient illumination conditions, the term bihemispherical reflectance (BHR), or blue-sky albedo, is used to describe albedo (Schaepman-Strub et al. 2006). In some cases, when the illumination is assumed to be completely isotropic, BHR is referred to as white-sky albedo (Lucht et al. 2000). Directional reflectance observations made from air- or spaceborne instruments cannot be directly converted to albedo, but information on the target's bidirectional reflectance distribution function (BRDF) is required (e.g. Ranson et al. 1991). The BRDF describes the angular anisotropy of reflected radiation. In the extreme cases of isotropic (or Lambertian) reflectance, the radiance reflected by the surface is the same for all viewing directions, whereas specular reflectance refers to surfaces that reflect radiation to the forward direction only (i.e. to the direction that forms the same zenith angle with respect to the surface normal, but has the opposite azimuth to the incident angle). Natural surfaces usually scatter radiation anisotropically, and a variety of models have been developed to describe their directional reflectance distribution (Strahler 1994). For example, surface anisotropy may be described using semi-empirical kernels that are weighted based on the volume scattering and geometric surface scattering effects of the particular surface (Wanner et al. 1995). The reflectance anisotropy of forests is typically strong and characterised by high reflectance in the backscattering direction (when the view and solar directions coincide, also known as hot spot) and low in the forward direction in the solar principal plane (e.g. Ranson et al. 1994; Deering et al. 1999). Ranson et al. (1994)

and Kleman (1987) noted that the reflectance anisotropy is dependent on species and stronger for spruce than for pine or broadleaved forests or for open vegetation. They discussed that the dense and clustered structure of spruce canopies could decrease radiation transmission and lead to an increased ratio of backward to forward scattering as compared to other vegetation types.

Surface albedo depends both on the wavelength and on the angular distribution of irradiance. To be able to examine the interactions between solar radiation and vegetation, it is thus important to understand the spectral and angular properties of the incident solar radiation. Of the extraterrestrial solar irradiance (~1366 W m^{-2}), ca. 50% is at wavelengths shorter than 0.7 µm, and 98% at wavelengths shorter than 3 µm (Gates 1980). The wavelength distribution of solar radiation transmitted through the atmosphere ranges from approximately 0.3 µm to 5 µm. Only a very small fraction of solar radiation at wavelengths shorter than 0.3 µm reaches the Earth's surface, as the molecular absorption of ultraviolet radiation by gases such as oxygen, ozone and nitrous oxide in the atmosphere is strong. Atmospheric absorption is small in the visible wavelength range (0.4–0.7 µm) (VIS). However, visible radiation is attenuated in the atmosphere due to molecular Rayleigh scattering, which is stronger the shorter the wavelength. Atmospheric absorption increases at near-infrared (0.7–1.3 µm) (NIR) and shortwave-infrared (1.3–5 µm) (SWIR) regions, mainly due to absorption by water vapour. Incident solar radiation can be divided into direct beam radiation that has not been scattered while passing through the atmosphere, and diffuse radiation that has been scattered once or several times before it reaches the surface. Diffuse radiation thus irradiates the surface from all angles of the hemisphere, but the intensity distribution of the diffuse radiation depends on the solar position as well as on atmospheric conditions (Kondratyev 1969). The sum of the direct and diffuse radiation is referred to as global radiation. In clear-sky conditions, most of the global radiation energy is in the direct beam radiation, but the proportion of diffuse radiation increases with increasing solar zenith angle (SZA). The vertical transmittance of a cloudless atmosphere varies in a wide range from 0.4 to 0.8 (Gates 1980). With increasing SZA, the path length and radiation attenuation increases and less direct beam radiation reaches the surface. Parallel to considering radiation as electromagnetic waves with specific wavelengths, radiation can also be thought to consist of discrete units, called quanta, or photons. The energy content of a quantum is determined by its wavelength.

Once a photon reaches the forest, it can either be absorbed by the canopy or ground, or it can be reflected back to the atmosphere. Absorption can occur at a photon's first encounter with a forest element, or the photon can be reflected or transmitted once or several times before it is absorbed. Likewise a photon can escape back to the atmosphere after it has been scattered (reflected or transmitted) once or several times within the forest. The likelihood of a photon being absorbed or scattered varies with the wavelength and depends on canopy structure and the optical properties of the forest elements. Reflectance and transmittance of leaves and needles is low in the visible spectral range, where photosynthetic pigments absorb radiation to drive the light reactions of photosynthesis. The wavelength range of visible radiation approximately coincides with the photosynthetically active radiation (PAR). Chlorophylls, the most abundant photosynthetic pigments, have their absorption peaks in the blue and red regions of the spectrum (Sims and Gamon 2002). Scattering is high in the NIR spectral domain, and serves to protect the leaves from excessive heating. SWIR absorption by the foliage is higher than that of NIR and is influenced by a leaf's internal structure and increased by increasing water content in the leaf tissues (Ceccato et al. 2001). Woody canopy parts are typically more reflective in the

visible and less reflective in the NIR spectral regions compared to the foliage (Roberts et al. 2004). Coniferous needles are often characterised by a lower single scattering albedo than the leaves of broadleaved trees (Gates 1965; Williams 1991; Roberts et al. 2004; Lukeš et al. 2013a).

When moving from the leaf to higher hierarchical levels (shoot, branch, canopy) the probability of photon absorption increases, and reflectance decreases (Dickinson 1983; Williams 1991; Roberts et al. 2004). The spatial arrangement of all the separate canopy elements in the forest affects the distribution of radiation and its pathways through the canopy (Norman and Jarvis 1974). For example, grouping of the foliage elements at any hierarchical level decreases the interception of radiation compared to a stand with a horizontally homogeneous distribution of foliage elements (Oker-Blom and Kellomäki 1983). Smolander and Stenberg (2003) showed that the clumping of needles into shoots decreases canopy interception compared to a leaf canopy when the leaf area index (LAI) is fixed. This decrease in canopy interception was accompanied by a decrease in forest reflectance when the canopy was bound underneath by black soil. Rautiainen and Stenberg (2005) discussed that the observed lower reflectances of coniferous forests compared to broadleaved ones could largely be explained by shoot-level clumping.

Forest reflectance properties can be changed by seasonal variation in the canopy and background conditions, such as leaf growth and fall or snow cover. If no snow is present, the deciduous forest reflectance has been observed to be highest prior to budburst and during senescence in the visible spectral domain, whereas reflectance in NIR is highest during midsummer when LAI is at its peak value (Kobayashi et al. 2007; Nilson et al. 2008). The understorey vegetation also undergoes seasonal changes that affect its spectral reflectance (Miller et al. 1997). Ground snow cover somewhat increases the albedo of both coniferous and deciduous broadleaved forests compared to the snow-free season (Betts and Ball 1997), while snow intercepted to the canopy has been suggested to either increase (Stähli et al. 2009) or have no effect on (Pomeroy and Dion 1996) coniferous forest albedo. Canopy snow interception refers to snow that accumulates on the branches and needles of the trees.

The influence of forest floor on forest reflectance depends on the canopy cover. Forest reflectance at small LAI and canopy cover may either be higher or lower than in a closed-canopy forest depending on whether the canopy is bound underneath by ground that is brighter or darker than the canopy (Ross 1981). However, abundant green understorey vegetation is common in boreal forests, and differences between the optical properties of the canopy and understorey may be small. This has been shown to complicate the retrieval of LAI or canopy cover from remotely sensed observations in boreal forests (Chen and Cihlar 1996; Miller et al. 1997; Gemmel 1999; Eriksson et al. 2006; Heiskanen et al. 2012). On the other hand, the contrast between the canopy and forest floor reflectance can be high in winter if the ground is covered with snow. The albedo of new pure snow can be higher than 0.8 (Gardner and Sharp 2010), but it is significantly reduced as the snow ages and grain size increases (Wiscombe and Warren 1980; Peltoniemi et al. 2005), or impurities accumulate on the snow surface (Melloh et al. 2001). Melting of snow additionally causes liquid water to fill the air between the grains, which increases the effective grain size and reduces the albedo of snow (Wiscombe and Warren 1980). Unlike vegetation, the reflectance of snow is higher in the visible than in the NIR spectral region (Wiscombe and Warren 1980; Peltoniemi et al. 2005).

It is generally assumed that spectral reflectance may be related to the structural variables of a forest stand. Remote sensing observations are used in many national forest

inventories (NFIs) to improve the accuracy and spatial representativeness of the forest resource estimates (e.g. McRoberts and Tomppo 2007). It is also common to use remotely sensed spectral data to infer information of the biophysical forest variables, such as LAI or the fraction of absorbed photosynthetically active radiation (fPAR), which can be directly linked to mass and energy exchange between the forests and the atmosphere (Ganguly et al. 2008).

1.4 Methods for estimating albedo

The albedo of a surface can be measured in the field using pyranometers or other equivalent sensors (e.g. Kondratyev 1969), which measure the energy of hemispherical irradiance in the solar wavelengths. Although air- and spaceborne instruments presently observe the Earth with higher temporal, spatial and radiometric frequency than previously, in-situ albedo measurements are still a routine part of the meteorological flux tower measurements (e.g. Betts and Ball 1997; Baldocchi et al. 2001; Hollinger et al. 2010). Permanent in-situ albedo measurements are valuable as, in addition to quantifying the shortwave energy balance of the flux measurement sites, they can be used for validating the satellite albedo products (e.g. Cescatti et al. 2012) and for observing long-term (Kirschbaum et al. 2011) or seasonal (Hollinger et al. 2010) trends in albedo. Albedo measurements using movable masts outside the maintained flux measuring sites are rare (but see Riihelä and Manninen 2008). Some studies have also used aircraft-mounted pyranometer measurements to obtain albedos of locally typical land cover types (Ben-Gai et al. 1998).

Albedo estimation from spaceborne observations has rapidly increased during the past few decades along with the introduction of new sensors. For example, observations from the Advanced Very High Resolution Radiometer (AVHRR) (Csiszar and Gutman 1999; Strugnell et al. 2001), geostationary Meteosat instrument (Pinty et al. 2000) and more recently from the Moderate Resolution Imaging Spectroradiometers (MODIS) (Schaaf et al. 2002) and Multiangle Imaging SpectroRadiometer (MISR) (Geiger et al. 2008) onboard the Aqua and Terra satellites, have been used to estimate surface albedo. Muller et al. (2012) estimated global albedo over a 15-year period using data from the European SPOT 4 and 5 satellites and from the MERIS sensor onboard the Envisat satellite. Quite recently, directional reflectance estimates calculated from the Landsat observations have been converted to albedos utilising surface BRDF approximations derived from MODIS data (Shuai et al. 2011; Román et al. 2013). Albedo retrieval from satellite observations includes uncertainty related to, for example, scattering and absorption of radiation in the atmosphere, sensor calibration, location issues, surface reflectance anisotropy and to the narrow- to broadband conversion of reflectance. Much used satellite albedo products today are those produced from MODIS observations. MODIS sensors acquire images on a wide across-track swath, and thus have a frequent global coverage. Over a 16-day period, the obtained multiangular reflectance observations are used to estimate surface albedo. The MODIS albedos have been validated against in-situ-measured albedos as well as albedo retrievals from other remote sensing instruments (Stroeve et al. 2005; Liu et al. 2009; Cescatti et al. 2012; Román et al. 2013; Wang et al. 2012; 2014). However, only a few studies have attempted to link forest albedo and its variation due to environmental and structural effects to remotely sensed albedo data (Jin et al. 2002; Davidson and Wang 2004; 2005; Bernier et al. 2011).

Forest reflectance modelling typically aims at understanding the spectral reflectance signal of forest vegetation and using this information for interpreting satellite-measured data (Nilson et al. 2003). Understanding radiation transfer in vegetation canopies has also been of importance for photosynthesis studies (Norman and Jarvis 1975). Recently, however, physically-based forest reflectance models have been modified and new ones developed to enable forest albedo estimation (Ni and Woodcock 2000; Wang 2005; Manninen and Stenberg 2009). Such models can be used to examine e.g. relationships between forest albedo and forest structure (Ni and Woodcock 2000; Lukeš et al. 2013b) or forest floor reflectance (Ni and Woodcock 2000; Manninen and Stenberg 2009).

1.5 Motivation and aim of the study

Forest albedo varies temporally and spatially due to, for instance, snow, phenology, tree species composition, forest structure and understorey composition. These factors in combination produce a continuous variation in forest albedo, and may be interrelated in a complex manner. For example, the effect of snow on forest albedo depends on whether snow covers the ground only or is also intercepted to the canopy. If snow is present on the ground only, the evergreen coniferous canopy tends to mask the snow and decrease the albedo compared to deciduous forests or open areas. On the other hand, coniferous forests with high LAI may intercept a considerable amount of snowfall to their canopy (Hedström and Pomeroy 1998), which may cause an increase in coniferous albedo with increasing LAI. The contribution of the forest floor on forest albedo depends on the canopy structure, which again may change the composition (Kuusipalo 1983; Hotanen et al. 2001) and fractional cover (Eriksson et al. 2006) of the understorey vegetation and thereby its reflectance. Stands with different tree species have been observed to have differing albedos (Betts and Ball 1997), but how are the species-specific albedos scaled in a mixed stand? Research on the variation in boreal forest albedo due to the above-mentioned factors is scarce. More research has been carried out to evaluate the effects of structural forest variables on the directional spectral reflectance of forests, as this kind of information is useful in interpreting remotely sensed data (e.g. Nilson et al. 2003). Such studies can aid in forming hypotheses and interpreting data of forest albedo, but cannot provide actual values of the shortwave radiative energy exchange.

From a practical point of view, important questions that can be asked include: Do stands of different tree species have different albedos? If so, how large are these differences, and how are they affected by seasonality, e.g. snow cover? Do species-specific albedos vary with forest structure and background properties, and how could this variation be quantified? Answers to these questions could, depending on the decision-makers' preferences, be used when considering the climatic effects of silvicultural options, such as the choice of tree species, rotation length, and harvesting options. Besides practical decision-making, accurate estimates of surface albedo are important for climate prediction and modelling, particularly in environments where climate warming is likely to cause albedo-related feedback mechanisms, such as snow albedo feedback in boreal regions.

The general aim of this thesis was to employ albedos estimated using in-situ pyranometer measurements, satellite albedo retrievals, and modelling to characterise temporal and spatial variation in Finnish boreal forest albedo. Spatial variation can be understood to represent the variation in forest albedo that is caused by changes in the structural and biophysical properties of forests in a landscape, whereas the temporal

dimension refers to seasonal or diurnal albedo variations. The theoretical background presented in the introduction guided the formulation of the hypotheses and specific questions: 1) It was assumed that snow cover increases forest albedo, but how large this increase is in a coniferous forest and what the role of canopy snow is on the forest albedo was unknown. The effect of snow on albedo was presumed to differ between land cover types, and the objective was to investigate the magnitude of these differences. 2) Forests of the most common Finnish tree species (Scots pine (*Pinus sylvestris* L.), Norway spruce (*Picea abies* (L.) Karsten) and birches (*Betula pendula* Roth. and *Betula pubescens* Ehrh.)) were thought to have different albedos during all seasons, and the albedo of forests of certain tree species was hypothesised to be affected by forest structure and understorey composition. The aim was to estimate the differences in species-specific albedos as well as to evaluate the effect of forest structure on albedo. 3) Based on the differences in forest albedo due to the above-mentioned factors, it was assumed that forest albedo could be modified by forest management. 4) The applicability of the different albedo retrieval methods was estimated.

2 MATERIAL AND METHODS

2.1 In-situ albedo measurements

In-situ albedo measurements can be considered the "reference" measurements against which satellite- or model-derived albedos can be evaluated. Naturally, even mast-measured albedos are not free of error; for example, sensor inter-calibration issues and error in the irradiance measurements, disturbing effects of the measuring system (reflectance or shadowing from the mast or other sensors), environmental factors such as dew, rain drops, insects, etc. on the sensors, and tilting of the mast in windy conditions may cause uncertainty to the data. Nevertheless, in-situ measurements are not influenced by the intervening atmosphere unlike remote sensing observations, nor do they suffer from the assumptions and simplifications needed in modelling. In-situ albedo measurements used in this thesis are based on the permanent radiation measurements of the Hyytiälä research station located in southern Finland (61°51´N and 25°17´E) (study I) as well as on measurements conducted using a movable telescopic mast in the vicinity of the station (study II). The purpose of study I was to examine the seasonal albedo variation of a boreal Scots pine forest. As only a few studies exist, which attempt to quantify the impact of canopy snow on forest albedo, let alone on the annual shortwave radiant energy balance, this aspect of the study was given special weig
ht. The objective of study II was to investigate the differences in albedo between forests of different 1) tree species, and 2) canopy structure within tree species.

2.1.1 Measurements at the Hyytiälä research station

Incoming and reflected shortwave radiation are measured as part of the routine measurements at the Hyytiälä research station. In study I, these measurements were utilised during a four-year period (2008–2011). During this time, incident solar radiation flux was initially measured using a Reemann TP-3 pyranometer (Astrodata, Tõravere, Tartumaa, Estonia) and a Middleton Solar SK08 pyranometer (Middleton Solar, Yarraville, Australia)

since June 2008. Reflected solar radiation was measured with a Reemann TP-3 pyranometer situated at a height of 70 metres on a measuring mast on a two-metre long boom. Snow and ice accumulation on the radiation sensors was prevented by fans placed next to the sensors. Digital photographs of the canopy were taken by an automated digital camera beginning from April 2008. The photographs were used to classify days into six classes based on the canopy snow interception. Snow-covered canopy was divided into four classes (1 = least snow, 4 = most snow) (Figure 1). Additionally, one class (0) was assigned to snow-free and one to frosted canopy (frost) (see study I for a more detailed description of the classes). Ground snow depth was measured on a weekly interval. The forest in the field of view of the downward facing pyranometer was a 50-year old stand dominated by Scots pine, with a minority of broadleaved deciduous species and Norway spruce reaching the canopy layer. The average effective leaf area index (LAI_e) of the site was 2.2, estimated from hemispherical photographs in 2011.

2.1.2 Albedo measurements using a telescopic mast

In-situ albedo measurements were carried out in the field in close proximity to the Hyytiälä research station during the summers of 2011– 2013. During this time, three Scots pine (P1–P3), three Norway spruce (S1–S3), one silver birch (B), and one (spruce) seedling stand (C) were measured. The criteria for choosing the measured stands were maximising the differences in canopy structure in stands of a certain species, while keeping the confounding factors (tree species mixture, variation in understorey vegetation) at minimum.

Figure 1. Canopy snow classes 1-4.

Table 1. Forest variable descriptions. Species (P. for Pinus and B. for Betula), stand density (trees/ha), mean height (m), mean DBH (diameter at 1.3 meter height, cm), length of the living crown (m), LAI (m^2m^{-2}), canopy cover and forest age (y) are presented.

	Species	Stand density	Height	DBH	Crown length	LAI	Canopy cover	Age
P1	*P. sylvestris*	3002	10.2	11.2	4.1	4.23	0.75	28
P2a	*P. sylvestris*	1053	13.2	15.1	6.4	3.63	0.74	35
P2b	*P. sylvestris*	559	13.7	16.6	6.9	2.15	0.41	35
P3	*P. sylvestris*	12127	2.3	1.7	-	1.26	0.16	14
S1	*Picea abies*	729	19.3	22.1	11	7.30	0.71	46
S2	*Picea abies*	398	19.9	25.4	12.4	3.80	0.40	68
S3	*Picea abies*	1924	8.8	9.8	7.8	4.77	0.63	22
B	*B. pendula*	979	14.3	13.1	8.1	3.55	0.73	28
C	*Picea abies*	2300	1.6	1.5	-	-	-	7

One of the pine stands (P2) was measured before (P2a) and after (P2b) a thinning, during which ca. 42% of the dominant trees were removed. According to Cajander's (1949) fertility-based site classification system, sites P1 and B belonged to the herb-rich *Oxalis-Myrtillus* -type, all spruce stands (S1–3) to the mesic *Myrtillus* -type, pine stand P2 to the sub-xeric *Vitis-idaea* -type and pine stand P3 to the xeric *Calluna* -type. Seedling stand (C) was covered by abundant grass and herbaceous vegetation. Radiation sensors (pairs of factory-calibrated Middleton Solar SK08 pyranometers and Apogee quantum sensors) measuring the incoming and reflected shortwave (0.3–3 µm) and PAR (0.4–0.7 µm) radiation were situated on a ca. one-metre long boom on top of a telescopic mast reaching approximately four metres above the canopy top. A pair of Middleton Solar SK08 sensors was additionally placed on a boom attached to a tripod at approximately a height of one metre to measure the incoming and reflected shortwave radiation beneath the canopy. Each stand was measured for a 1–3 week period in June–August. Forest variables within 95% of the signal area (ca. 465 m^2) are shown in Table 1. Effective LAI (LAI_e) and canopy cover were estimated from hemispherical photographs, and the LAI_e values were divided by the empirical shoot-level clumping indices of 0.59 for pine (Smolander et al. 1994) and 0.64 for spruce (Stenberg et al. 1995) to yield an estimate of true LAI (Table 1). These true LAI values could still be underestimates due to foliage clumping on higher hierarchical levels than the shoot level.

Daily albedos were calculated for all in-situ measurements as the ratio of the sum of daily (SZA<90°) reflected solar radiation to that incident on the canopy. Daily albedo calculated this way quantifies the fraction of total solar irradiance leaving the surface that day, and is suitable for energy balance studies. For estimating albedo during clear skies or overcast conditions only, the sky was classified as overcast when the measured solar radiation totalled less than 50% of that in typical clear-sky conditions. Understorey albedos in study II were computed only for days that were completely overcast throughout the day.

2.2 Utilisation of remotely sensed data

Remote sensing observations are typically used to complement labour-intensive and thus expensive field measurements. Either statistical or physically-based models are employed to derive spatially representative estimates of the ground-measured or -estimated variables. The field-measured albedo data set was small in this thesis, and the main interest in using

satellite albedo products was to obtain information that was spatially more representative than that measured in the field, as well as to compare this information to the small set of measured albedos. The MODIS albedo product used in studies III and IV has a considerably larger spatial resolution (25 ha) than a typical homogeneous forest management unit (not more than a few hectares in southern Finland). Thus, instead of directly comparing pixelwise albedos with land cover types or forest variables within those pixels, regression analyses using the abundances of the different land cover components as predictors and the MODIS pixel albedos as response variables were conducted. This "linear unmixing" -method facilitates the estimation of the component albedos. We were specifically interested in the albedo differences between various land cover types and tree species or species groups, and on the seasonal development of the land cover type-specific albedos (study III). The unmixing method was revised in study IV to account for species-specific changes in albedo with forest age. Albedos estimated from Landsat observations using the method proposed by Shuai et al. (2011) were used to provide a comparison for the albedo-age relationships obtained from the unmixing analysis of MODIS albedo retrievals.

Studies I– IV do not provide the possibility of properly examining the variation in forest albedo or reflectance separately as a function of various forest structural variables or understorey properties. This step was taken in study V, where Landsat-derived surface directional reflectances and a comprehensive set of field data from the 10th and 11th NFIs were used to study the dependencies of the spectral reflectances on the forest variables, as well as to use nonlinear unmixing analysis to estimate understorey- and canopy-specific reflectances.

2.2.1 MODIS and Landsat albedos and Landsat BRF

MODIS albedo retrievals (MCD43A3, collection 5) with 500 m × 500 m spatial resolution downloaded from (ORNL DAAC 2012) were used in studies III and IV. The MODIS albedo algorithm uses atmospherically corrected observations of surface directional reflectances that are collected over the 16-day aggregation periods (Schaaf et al. 2002). These observations are used to fit a kernel-based BRDF model to yield surface BRDF parameters (Lucht et al. 2000). Directional-hemispherical (DHR, or black-sky) and bihemispherical (BHR, or white-sky) albedos as well as blue-sky albedo at local solar noon are then estimated in 8-day intervals for the seven spectral bands (Lucht et al. 2000; Román et al. 2010). Narrow to broadband conversion coefficients (Liang 2001) are used to compute the broadband visible (0.3–0.7µm) (VIS), near- and shortwave infrared (0.7–5.0 µm) (NIR_m) and shortwave (0.3–5.0 µm) (SW) albedos. Each of the seven spectral bands used in the albedo estimation of each pixel is given a quality flag based on the number and angular distribution of the cloud-free observations acquired during the aggregation period. Study III utilised four years of good quality albedo retrievals from both study locations, whereas only two good quality samples covering the study area in winter, spring and summer were used in study IV.

Landsat 5 TM images used in studies IV and V were acquired on 29th June 2011 from path 190 and rows 16–17 (study IV) and rows 13–17 (study V). In both studies, the surface bidirectional reflectance factors (BRFs) were first estimated from the Landsat-measured radiances using the atmospheric correction code LEDAPS (Masek et al. 2006). Bidirectional reflectance factor (BRF) refers to the ratio of the radiant flux reflected from a surface to that reflected from a Lambertian surface at the same illumination and viewing angles (Shaepman-Strub et al. 2006). In study IV, albedo was estimated from the Landsat

BRFs following the method developed by Shuai et al. (2011). Landsat observations cannot be used to characterise the surface reflectance anisotropy, and thus BRDF parameters derived from the MODIS BRDF/albedo product were used for this purpose. The albedos were estimated for the same broadbands as for MODIS. In study V, only the nadir view BRFs in the Landsat red (0.63–0.69 µm), NIR (0.76–0.9 µm) and SWIR (1.55–1.75 µm) wavebands were used.

2.2.2 Land cover and forest resource data

Land cover information was needed to define the components and their abundances in the unmixing models (section 2.4) in studies III and IV. The land cover and forest resource estimates produced in the Finnish multi-source NFI at the Finnish Forest Research Institute (Tomppo and Halme 2004; Tomppo et al. 2008b) were employed in both studies. The raster data with 20 m × 20 m spatial resolution included estimates of land cover and forest variables (e.g. land class, site fertility, stand age, species-specific volume of growing stock), that were produced using field measurements of the Finnish NFIs, digital map data and Landsat TM or ETM+ images with an improved version of the non-parametric k-NN method (ik-NN) (Tomppo and Halme 2004; Tomppo et al. 2008b). In study III, land cover-type specific albedos were estimated for an area surrounding the Hyytiälä research station, using altogether 5088 MODIS pixels. In study IV, the study area was larger but only the MODIS pixels belonging completely to the land class "forest land" were used in the analysis. Forest land included productive forests both on mineral and peatland soils. The data in study IV was further divided into training and test data by random sampling, comprising 80% and 20% of the total of 2180 MODIS pixels used in the analysis, respectively.

Additional land cover data (©Metsähallitus 2012) from eastern Finnish Lapland (Värriö) (67°48´N, 27°52´E) were used in study III. The data were in a vector format from which they were converted into rasters on 20-m grids. The data included qualitative land cover information of all land cover types.

Field plot measurements carried out as part of the 10th and 11th Finnish NFIs were used in study V. The data were filtered so that only monospecific plots with only one tree layer were included, with at least 20 m to the nearest stand boundary and located on mineral soils. Young seedling stands (mean height <1.3 m) and stands that had undergone selective regeneration cuttings were additionally removed. The canopy cover estimates in the inventory data were partly estimated in the field and partly modelled.

2.3 Albedo modelling

The forest albedo model PARAS (Manninen and Stenberg 2009) was used to estimate field plot albedos in the total shortwave and PAR spectral regions in study II. The model was additionally used to estimate the amount of multiple-scattered radiation from the tree canopy that contributed to the sunlit understorey reflectance, required in the nonlinear unmixing analysis in study V (section 2.4). The PARAS albedo model is based on the spectral invariants theory (Knyazikhin et al. 2011). The model is fairly simple and computationally efficient, and requires only a few input parameters. It is specifically designed for albedo modelling, and thus requires no separate integration of directional reflectance values. The model employs a wavelength independent parameter p (photon

recollision probability) that describes canopy structure by the probability that a photon, once scattered from a canopy element, interacts within the canopy again (Smolander and Stenberg 2005). Using information on p and on the leaf (or needle) spectral albedo, the model can estimate canopy absorptance and scattering at any wavelength. The fraction of backward scattering (Q) defines the proportion of scattered radiation that is reflected back to the direction of incidence (Mõttus and Stenberg 2008). Additional model input parameters are directional gap fractions (t_0), diffuse non-interceptance (*DIFN*) and understorey, foliage and sky irradiance spectra.

Parameters LAI_e, t_0 and *DIFN* were estimated in study II from the hemispherical photographs taken on each study plot using the Hemisfer software (Schleppi et al. 2007) and the approach similar to that used in the LAI-2000 Plant Canopy Analyzer (LI-COR 1992). True LAI was estimated from LAI_e as explained in section 2.1.2.

LAI was calculated in study V from plot-wise foliage biomass estimates (Repola 2009) using specific leaf area values from Stenberg et al. (1999) and Palmroth and Hari (2001). LAI was increased to also take into account the woody canopy components using the branch to leaf area ratios suggested by Nilson (1999). Parameters t_0 and *DIFN* were estimated using the Lambert-Beer's law for radiation transmission adapted for vegetation canopies as in Manninen and Stenberg (2009). The nadir gap probability (t_{cc}) used in the unmixing analysis in study V was estimated directly from the canopy cover estimates given in the field plot data.

Leaf and needle spectral albedos used in the modelling were obtained from the measurements of Lukeš et al. (2013a), the reflectance spectra of woody canopy components from Lang et al. (2001) and the understorey spectra used in study II were measured in a similar way as those in Rautiainen et al. (2011). The understorey spectra (herbrich, mesic, sub-xeric and xeric) were adjusted in study II to match the measured understorey broadband shortwave albedos by multiplying by a constant factor over all wavelengths. Black-sky (Thuillier et al. 2003) and white-sky irradiance spectra were used to weight the spectral albedos produced by the PARAS albedo model to yield broadband albedos.

2.4 Linear and nonlinear unmixing

Spectral mixture analysis is a widely used method for estimating subpixel fractional covers (abundances) of land cover components with known spectra (endmembers) (e.g. Somers et al. 2011). Spectral mixture modelling can be either linear or nonlinear, depending on whether multiple scattering is assumed to occur between the image components (nonlinear) or not (linear). Linear mixture analysis is based on the assumption that each photon reaching the sensor has interacted only with one land cover component, and therefore that the pixel radiance recorded by an Earth-observing instrument is a linear combination of the surface component reflectances in the pixel field of view (Settle and Drake 1993). Contrary to the problem described above, the purpose here was to estimate the albedo (or reflectance) of land cover components whose abundances were known:

$$A = \sum_{i=1}^{n} f_i \, a_i + \varepsilon, \text{ where } \sum_{i=1}^{n} f_i = 1 \quad (1)$$

Here, A is the pixel albedo, n is the number of land cover components, f_i is the fractional cover (abundance) of component i in the pixel area, a_i is the albedo of that component and ε is the residual error. This approach was applied in studies III and IV, where land cover

albedos were estimated by predicting the MODIS blue-sky albedos by the component abundances using least squares regression. The fractional covers of the tree species in the Hyytiälä study area were estimated as their share of the total growing stock within a pixel. In study IV, we further assumed that the species-specific albedo varied as a function (p) of stand age:

$$A = \sum_{i=1}^{n} \frac{\sum_{k=1}^{j} f_{i,k} p_i(x_k)}{j} + \varepsilon, \quad (2)$$

where x_k is forest age in land cover pixel k, and $f_{i,k}$ the fractional cover of species i in that pixel. Notice that stand age was set to zero if no growing stock estimate for the land cover pixel existed. Exponential functions were used to model the change in forest albedo as a function of stand age. Separate models (p_i) were estimated for pine and spruce in summer, spring and winter, and for broadleaved deciduous species (mainly birch) in winter. Model parameters could not be estimated for the broadleaved species for summer and spring, and thus broadleaved component albedo was estimated as the mean albedo of the species, independent of age. The initial albedo (albedo of seedling stand) in winter was kept constant for all species. Exponential species-specific regressions were also evaluated for the Landsat summer albedo retrievals directly by choosing only Landsat pixels that were dominated by one tree species (> 90%). Regressions for spruce SW and NIR_m albedos were estimated only for stands older than 10 years, as the spruce stand albedo actually increased before this. Possible reasons for this are discussed in section 3.2.2. Both the functions estimated by unmixing from the MODIS albedos and those estimated directly from the Landsat albedo data were used to predict the MODIS test data set albedos. The test data albedos were additionally predicted using only species-specific mean albedos and the albedo of a clear cut estimated from MODIS data by unmixing (Eq. 1).

The interest of the unmixing analysis in study V focused on the understorey BRFs and their development during stand succession. The forest scene was assumed to be composed of two spectrally distinct components, namely "sunlit understorey" and "canopy and shaded ground". In the absence of multiple scattering between the components, the fraction of the "sunlit understorey" could be estimated as $f_u = t_0 \times t_{cc}$ (t_0 is the gap fraction in the solar and t_{cc} in the sensor direction, see section 2.3) and the fraction of the "canopy and shaded ground" component as $1\text{-}f_u$. In the presence of green vegetation with high NIR reflectance, it is however likely that multiple scattering between the components violates the linear mixing assumption (e.g. Chen and Vierling 2006; Somers et al. 2009). The PARAS albedo model was therefore used to estimate the radiation component that reaches the sunlit understorey after first interacting with the canopy. The spectral BRFs of the "sunlit understorey" and "canopy and shaded ground" components were estimated from Landsat data as:

$$BRF = \sum_{k=1}^{m} a_{ck} f_{ck} + \sum_{k=1}^{m} \sum_{j=1}^{n} a_{ujk} f_{ujk} + \varepsilon \quad (3)$$

BRF is the Landsat bidirectional reflectance factor, f_{ck} is the fraction of the "canopy and shaded ground" component in stand development class k, and f_{ujk} is the fraction of the "sunlit understorey" component in stand development class k and site fertility class j within a Landsat pixel. The component fractions summed up to one within a pixel and each plot

represented only one class of stand development and site fertility. Parameters a_{ck} and a_{ujk} are the respective BRFs of the "canopy and shaded ground" and "sunlit understorey" components, and ε the residual error. Due to the low number of pure spruce plots (70), the stand development class could be included in the estimation of the component BRFs in pine stands (954) only. The stand development classes used in the analysis were "mature seedling stand" (DC3), "young thinning stand" (DC4) and "advanced thinning and mature stand" (DC5+6). The site fertility classes were *Oxalis-Myrtillus* (OMT), *Myrtillus* (MT), *Vitis-idaea* (VT) and *Calluna* (CT) (in order of decreasing fertility). The term "understorey" here refers to all forest floor vegetation as well as non-vegetated surfaces.

3 RESULTS AND DISCUSSION

3.1 Temporal variation in albedo

Seasonality of albedo was examined in studies I, III and IV, and the diurnal albedo cycle was considered in study II. The diurnal course of clear-sky albedo during the snow-free season was bowl-shaped at all field measurement sites where completely sunny days occurred. This form of diurnal albedo course has been widely reported in the literature (e.g. Stewart 1971; Lafleur et al. 1997; Ni and Woodcock 2000; Deering et al. 1999), and may be caused by the high backscattering of beam radiation from the canopy tops and a low transmittance of radiation to the forest when the sun is close to the horizon. At very high solar zenith angles (> 85º), the albedo may again begin decreasing due to the high fraction of diffuse radiation from the total irradiance (Ni and Woodcock 2000). On overcast days, albedo was stable throughout the day, which can be explained by the more even angular distribution of incoming radiation than during clear-sky conditions (Ni and Woodcock 2000). In a simulation of black spruce red band albedos in completely direct (DHR) and diffuse (BHR) conditions, Shaepman-Strub et al. (2006) found that BHR, which was independent of SZA, was higher than DHR at SZAs lower than ca. 55º, and lower at SZAs higher than 55º. The midday albedos observed at our study sites in summer (study II) were similar in clear- and overcast-sky conditions. This, together with the fact that the overcast days lacked the higher morning and evening albedos, resulted in higher daily albedos measured during clear or all sky conditions than in overcast conditions. Interestingly, no differences were observed in the daily PAR albedos between all sky and overcast conditions in the in-situ measurements (Table 2) despite the bowl-shaped course of PAR albedo on the clear days. However, midday PAR albedos were higher in diffuse than in clear-sky conditions, in agreement with the results of Shaepman-Strub et al. (2006). The higher midday PAR albedos in diffuse conditions could compensate for the higher morning and evening PAR albedos in clear-sky conditions, and explain the similar daily PAR albedos in clear (or all sky) and overcast conditions.

Pine forest albedo measured at the Hyytiälä research station was fairly stable in summer, but varied considerably during seasons when snow cover occurred. The duration of the snow-covered period varied between years; permanent snow cover fell between mid-November and mid-December. Each year, the ground snow pack was thickest in mid-March and had melted by the end of April. Figure 2 shows the monthly means of the daily albedos when the canopy is assigned a certain snow class (0 = no snow, 1–4 = least to most snow). The albedo of a pine forest showed only little variation when the canopy was snow-

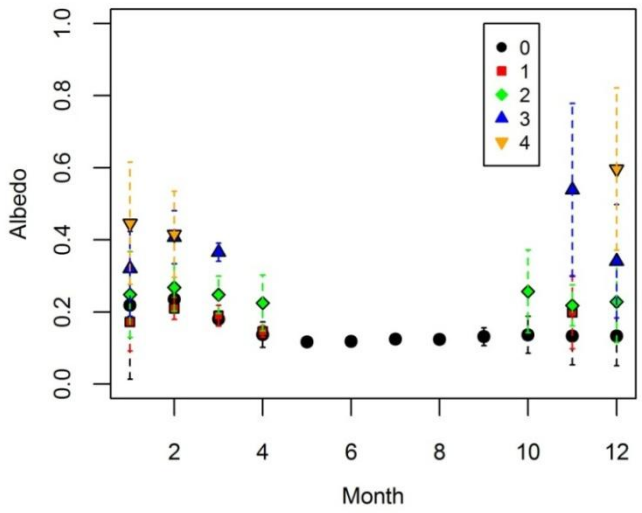

Figure 2. Monthly means of daily albedos when the canopy is assigned to snow classes 0–4 (0 = no snow, 1 = least snow, 4 = most snow).

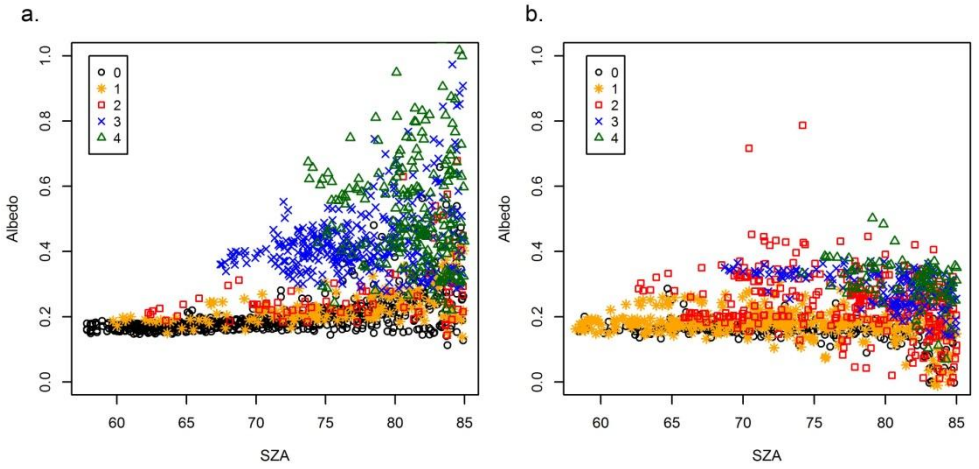

Figure 3. Albedo as a function of SZA and canopy snow class in January–March in a) clear-sky and b) overcast conditions.

free and the ground only periodically covered with snow in October–December. It is possible that the occasional shallow snow cover in early winter was effectively masked by the evergreen coniferous canopy. When ground snow cover became permanent and increased in depth in January–March, forest albedo increased almost twofold in the absence of canopy snow and threefold when the canopy was snow covered (snow class 1–4), compared to snow-free conditions. A small amount of snow in the canopy did not affect the

albedo (Figures 2 and 3), but as more of the branches and shoots became covered with snow, the albedo increased, particularly in clear-sky conditions.

The magnitude of the canopy snow pack alone did not explain all variation in the measured albedo. It was observed that a fall of new snow increased the albedo, but the high albedo rapidly decreased if no new snowfall occurred. This was likely due to the fact that snow ageing increases snow grain size, which decreases snow albedo (Wiscombe and Warren 1980). For example, a decreasing linear relationship between snow albedo and days after the last snowfall was reported by Baker et al. (1990). The albedo of a snow-covered forest correlated negatively with air temperature and incoming longwave radiation, which could be explained by the following reasons. SZA was high during periods of heavy canopy snow load, and on clear days, occurring together with cold air temperatures in winter, the high albedo could be due to high SZAs. The highest albedos were observed in clear-sky conditions when the canopy snow class was high (Figure 3), and it is possible that the assumed strong backscattering of the direct beam radiation at high SZAs would be further enhanced by the thick canopy snow pack. The metamorphosis of snow, and thus the increase in grain size, is additionally slower the colder the temperature (Taillandier et al. 2007). Contrastingly to our results, Betts and Ball (1997) measured higher albedos of snow-covered grasslands and forests in diffuse rather than in clear-sky conditions in Canada. They discussed several possible reasons for their observation. They mentioned that fresh snow with high albedo is more likely to occur in overcast conditions directly after snowfall. They also discussed that the wavelength distribution of irradiance under overcast-sky conditions, which is known to be slightly richer in visible wavelengths than that under clear skies (Jacovides et al. 2007; Mõttus et al. 2012), could be one reason for the higher snow albedo in overcast-sky conditions. However, the high albedos of the snow-covered canopy measured in this study were concentrated to the midwinter months with high SZAs, which could explain the difference to results obtained at more southerly latitudes. A frosted canopy appeared to have albedos comparable with those of the lowest canopy snow classes. Frost-covered needles could have higher albedos than unfrosted ones, but frost, unlike snow, does not fill the small canopy gaps and thus better permits radiation transmission into the canopy than a heavy snow pack.

Similar seasonal patterns as those measured from the Hyytiälä pine forest were obtained from the unmixing analysis of the MODIS albedo retrievals. Figure 4 shows the seasonal course (averaged over four years) of albedo in the Hyytiälä and Värriö study areas. In the Hyytiälä area, the intra-annual variation in albedo was lowest in the spruce and pine forests, while the largest seasonal differences were seen in water bodies and croplands. It is rather straightforward to interpret this to be attributable to the visibility of snow; highly reflective snow is not masked by tall and dense vegetation in frozen lakes and agricultural fields like it is in the evergreen spruce and pine forests. For the same reason, deciduous forests and seedling stands were found to have intermediate winter albedos. However, snow interception to the canopy, as discussed above, should increase the albedo of evergreen coniferous forests where the snow sticks to the branches and needles. A high canopy snow cover was evident at least in Värriö, where the spruce and pine forests received albedo values as high as or higher than the deciduous forests, close to 0.5 and 0.4 in midwinter, respectively. Forest albedos were rather stable in all study areas during the snow-free season, but albedo was somewhat higher in midsummer than in spring or autumn, particularly in deciduous broadleaved forests in the Hyytiälä area. This was probably caused by the higher NIR reflectance of deciduous broadleaved species in midsummer when LAI is high and the leaves fully developed. Nilson et al. (2008) also observed that

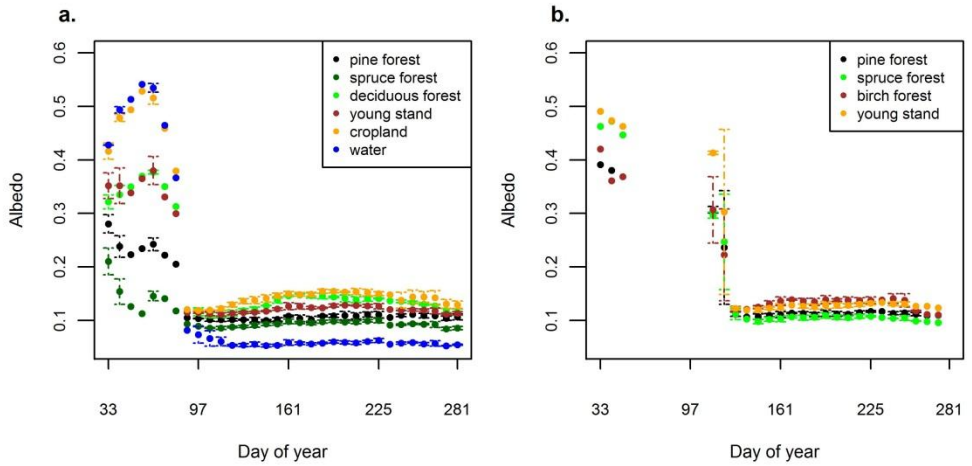

Figure 4. Seasonal albedo variation estimated from MODIS albedo retrievals in a) Hyytiälä, and b) Värriö study areas.

the NIR reflectance of Estonian birch forests estimated from Landsat observations was highest during the midsummer period, but reflectances in the visible wavebands were lowest during this time. The small changes in coniferous forest albedo during the snow-free season observed here could be caused by the phenology of the deciduous understorey vegetation (Nilson et al. 2008) and perhaps by differences in optical properties of the old and new needles (Rock et al. 1994). Changes in SZA likely additionally influence the seasonal course of albedo.

Ground and canopy snow cover increased the forest albedo measured at the Hyytiälä research station, and thus decreased the total amount of solar radiation annually absorbed by the forest as compared to a hypothetical snow-free winter (with a fixed albedo of 0.106). However, the canopy snow interception was generally large only during the midwinter months (Figure 5). The number of days in March when the canopy was covered with snow drastically decreased from that of January or February; during March and April snow was only retained in the canopy for short periods after a snowfall event. The decrease in canopy snow interception with proceeding spring is a result of increasing irradiance and air temperature. Increasing temperatures not only melt the snow, but also weaken the cohesion between the branches or needles and snow and cause snow to fall. High irradiance drives the sublimation of intercepted snow and can also accelerate the falling of snow by warming the branches and needles. Pomeroy et al. (1998) suggested that ca. one third of the annually intercepted snow can be lost by sublimation in a mature pine stand in Canada. In addition to the decreasing canopy snow interception, the properties of ground snow change during the course of the spring; snow melting and ageing due to increased temperatures and less frequent snowfall events lead to increased snow grain size and decreased albedo. In addition, impurities, such as litter and soot, accumulate on the surface and the snow depth decreases. It was accordingly observed that the albedo of the Hyytiälä pine forest with snow-covered ground decreased from January–February to March and April with equal canopy snow class. Because canopy snow interception rapidly decreased and ground snow albedo decreased as the irradiance increased during spring, the effect of snow on the annual

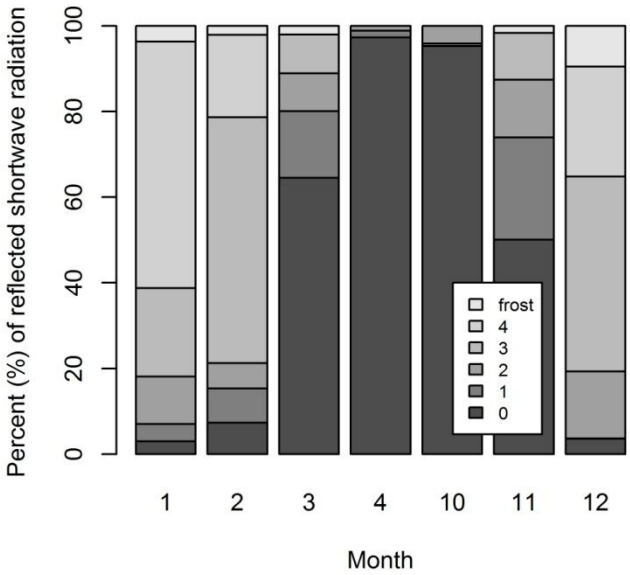

Figure 5. Percentage of days in each canopy snow class in each winter month.

shortwave energy budget of the forest was rather small. The difference between the total amounts of solar radiation reflected during an average winter (November–April) and a hypothetical winter with no snow either on the ground or in the canopy was 55 MJ m^{-2}. This accounted for ca. 2% of the annual irradiance, and was within the limits of the inter-annual variation of the total annual irradiance at the site. However, although the annually averaged effect of snow cover was small quite, its influence on the forest's radiation balance was important during the winter months.

3.2 Albedo and forest structure

3.2.1 In-situ albedo measurements

In-situ mast measurements of forest albedo were carried out in the surroundings of the Hyytiälä research station to investigate the between and within tree species variation of forest albedo. Forest structure was quantified by LAI, which was estimated from hemispherical photographs. In one pine stand (P2), albedo was measured before (P2a) and after (P2b) a thinning operation, during which nearly half of the dominant trees were removed. The measured albedo was highest in seedling stand C and birch stand B, followed by the pine (P1–P3) and spruce stands (S1–S2) (Table 2, Figure 6). The albedo of young spruce stand S3 was as high as those of the pine stands. No clear differences in shortwave albedo were observed between pine stands P1, P2a and P2b despite the differing LAI and canopy cover. The same was true for the two mature spruce stands S1 and S2. Within species differences in shortwave albedo were only evident when also considering the young pine and spruce stands P3 and S3. These two stands were, however, clearly different with

regard to the older stands. P3 was a seedling stand with a large proportion of visible ground due to small trees and a grouped tree distribution; the dry sandy soil was covered with patches of lichens, moss, bare soil, litter and heather (*Calluna vulgaris*). Contrastingly, stand S3 was a dense, ca. 9-metre spruce stand with a continuous moss understory. PAR albedo was also fairly insensitive to LAI within species; it decreased with increasing LAI in pine, but not in spruce stands. All spruce stands had, however, rather high LAIs and it is possible that the PAR reflectance had already been saturated. A peculiar increase in PAR albedo was observed after the thinning of P2 (Table 2). It was suspected that this increase could be caused by the side effects of harvesting, such as understorey vegetation (mainly dwarf shrubs) trampling by the harvester and by parts of the understorey vegetation being covered by piles of logging residues (branches). The stand was measured therefore again the same time next year, and PAR albedo had indeed decreased back to its pre-thinning level. Because harvesting did not affect the shortwave albedo, NIR albedo should proportionately have decreased as a result. Note that we did not measure NIR albedo but only shortwave and PAR albedos. An increase in the PAR and decrease in the NIR understorey albedo following a thinning is consistent with the results of Nilson et al. (2001), who measured understorey spectra in Swedish pine stands thinned to varying degrees and noticed a post-harvest increase in red band and a decrease in NIR reflectance. Similar but smaller changes in post-thinning reflectances at the stand level were noted by Olsson (1994) from Landsat observations. Nilson et al. (2001) argued that the changes in understorey reflectance were likely attributable to cutting residues. However, the temporal scale of our study is not directly comparable to the studies by Nilsson et al. (2001) or Olsson (1994), because they did not assess the reflectance immediately after the harvest, but at earliest one year after. After this, Olsson (1994) observed that the thinning caused change in reflectance diminished over time. Technical problems leading to errors in measurements, such as uncertainty in the irradiance measurements, mast tilting, sensor shadowing, backscattering from the mast, etc. cannot naturally be completely ruled out from our results. Nevertheless, the uncertainty related to the harvesting effects on understorey reflectance indicated that future experiments trying to evaluate the effect of managing forests at different densities on forest albedo should rather measure stands with a similar species composition in the over- and understorey, but different LAI and canopy cover.

Table 2. Measured average daily shortwave, PAR and understorey shortwave albedos (± standard deviation) for all-sky and overcast conditions. P2b* denotes stand P2b measured again during the following summer.

	Albedo		PAR albedo		Understorey albedo
	All sky	Overcast	All sky	Overcast	Overcast
P1	0.114±0.008	0.103±0.011	0.031±0.003	0.031±0.003	0.174± 0.007
P2a	0.115±0.009	0.107±0.008	0.034±0.002	0.034±0.003	0.124± 0.008
P2b	0.112±0.006	0.106±0.005	0.051±0.002	0.050±0.004	0.124± 0.008
P2b*	0.110±0.002	0.107±0.002	0.034±0.001	0.034±0.002	0.138±0.015
P3	0.129±0.005	0.120±0.013	0.037±0.001	0.037±0.001	0.103±0.007
S1	0.082±0.004	0.075±0.007	0.022±0.002	0.022±0.003	0.161± 0.018
S2	0.080±0.004	0.077±0.005	0.023±0.002	0.023±0.001	0.160±0.005
S3	0.114±0.005	0.106±0.007	0.026±0.001	0.026±0.001	0.162± 0.025
B	0.175±0.006	0.167±0.004	0.028±0.004	0.027±0.003	0.185±0.009
C	0.184±0.011	0.177±0.009	0.046±0.002	0.046±0.003	-

Understorey albedo measurements indicated that some of the insensitivity of the canopy level albedos to LAI could be due to the opposing effects of understorey albedo. For example, in P1, where LAI was higher than in P2 but the shortwave albedos were similar, the understorey albedo was higher than in P2. Understorey albedo was furthermore fairly low in thinning stand P2, which could diminish the increase in albedo following a decrease in the absorbing foliage biomass. Note that the understorey albedo at site P2 was measured from a spot that remained undisturbed during harvesting, and represents a mean of the measurements carried out before and after the thinning. These assumptions on the compensating effects of the understorey were reinforced by results gained from the albedo modelling: when the understorey spectra used in the modelling were adjusted by the measured understorey albedos, the model produced approximately equal albedos for sites P1, P2a and P2b (Figure 6). Due to the very low understorey albedo in P3, the modelled shortwave albedo of the site was even lower than those of sites P1–P2. The modelled PAR albedo was, on the other hand, higher for P3 than for P1–P2 because the xeric understorey spectra used to model the stand's albedo had a higher reflectance in the visible wavelengths than the spectra used at the other sites, and the understorey spectra were adjusted to match the measured albedos using a constant coefficient throughout the spectra, i.e. not in a wavelength-dependent manner. However, the understorey albedos were almost identical (and not particularly low) in all spruce stands, and thus neither the similarity of the shortwave albedos of stands S1 and S2, nor the high albedo of stand S3, could be explained by the understorey. Due to the similar understorey albedos of the spruce stands, the modelled albedos showed a decreasing trend with increasing LAI (Figure 6). However, it is once again important to be aware that the understorey albedo was measured only in one spot within each plot, and can thus provide a biased estimate of the stand's understorey albedo. Overall, the results showed that the albedo of understories with a considerable proportion of mosses and dwarf shrubs (P2–3, S1–3) were lower than those dominated by grasses, herbs and litter (P1, B, C).

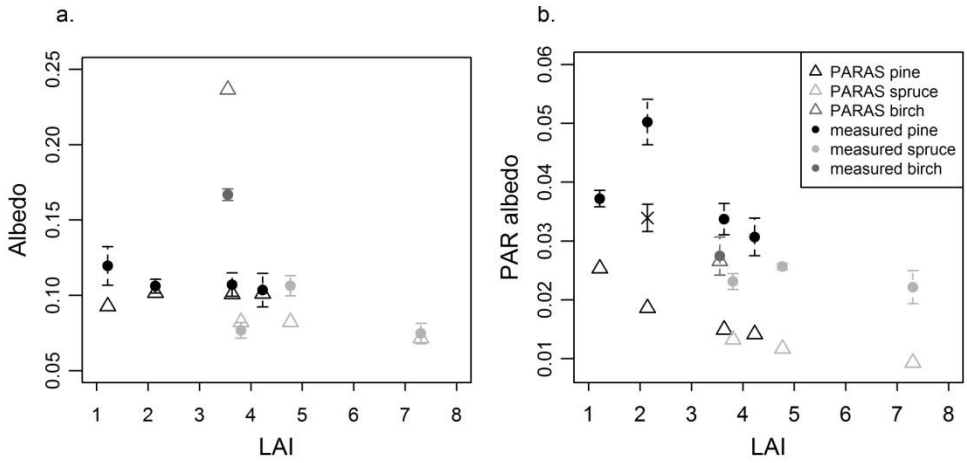

Figure 6. Measured (±standard deviation) and modelled (PARAS) shortwave and PAR albedos. × is the PAR albedo measured at site P2b during the summer following the thinning.

Some hypotheses can be presented to explain the unexpectedly high shortwave albedo of young spruce stand S3. This high albedo was attributable to the NIR region, as the understorey and PAR albedos were fairly similar to those in the other spruce stands. Firstly, the proportions of canopy elements with different optical properties could vary between young and mature stands. For example, Rock et al. (1994) observed that first-year red spruce needles averaged higher reflectance than the second-year needles. If this would also hold for Norway spruce needles, the larger proportion of first-year to all needles in a young stand where the total needle mass is still increasing might explain the higher albedo of S3 compared to S1 and S2. Moreover, in mature stands S1 and S2, the contribution of woody canopy components, with generally lower NIR reflectance than that of the foliage, to albedo could be higher than in young S3. Other possible explanations include between stand differences in canopy or crown structure, such as tree height, crown shape, branch structure and orientation and tree density.

3.2.2 Analysis of remotely sensed albedos

The sample size of the in-situ albedo measurements was small and thus the measurements were not representative of the forests in the area. Examination of forest albedo variation was therefore continued in study IV using satellite-derived data. MODIS albedo retrievals provide validated and widely used data on land surface albedo, but the large pixel size (ca. 500 m × 500 m) is problematic if the objective is to compare forest variables and pixel albedo values in a fragmented landscape. We therefore employed the linear unmixing approach in study IV to infer forest albedo dependencies on stand age. This aim was met by estimating species-specific nonlinear (exponential) regressions describing albedo dependency on stand age in winter, spring and summer. Separate functions were estimated for the MODIS VIS, NIR_m and SW broadbands (Figure 7). Similar exponential regressions were estimated for the Landsat-retrieved summer albedos in the comparable broadbands.

Forest age is not a biophysical variable that could be directly related to forest albedo via some physically-based relationship, such as LAI. Forest albedo can nonetheless be assumed to depend on stand age due to some co-occurring changes in forest structure and species composition. Nilson and Peterson (1994) observed that coniferous forest reflectance in red and NIR wavebands decreases rapidly at young stand ages along with an increase in LAI and canopy closure in Estonian sub-boreal forest; the reflectance becomes more or less stable after the maximum canopy closure and LAI are reached at ca. 20–40 years of age. The authors suggest that the main reason for the strong decrease in reflectance during early succession would be the decrease in the fraction of sunlit ground vegetation. Another reason for the sharp initial decrease in the directional reflectance or albedo to be encountered in maturing managed coniferous forests is the decline in the fraction of deciduous broadleaved tree mixture (Amiro et al. 2006). The canopy cover and LAI may once again begin to decline in old coniferous forests. However, managed forests are usually harvested before the old growth stage. An advantage of using forest age as the predictor variable in an albedo model is that it is usually known in managed forests.

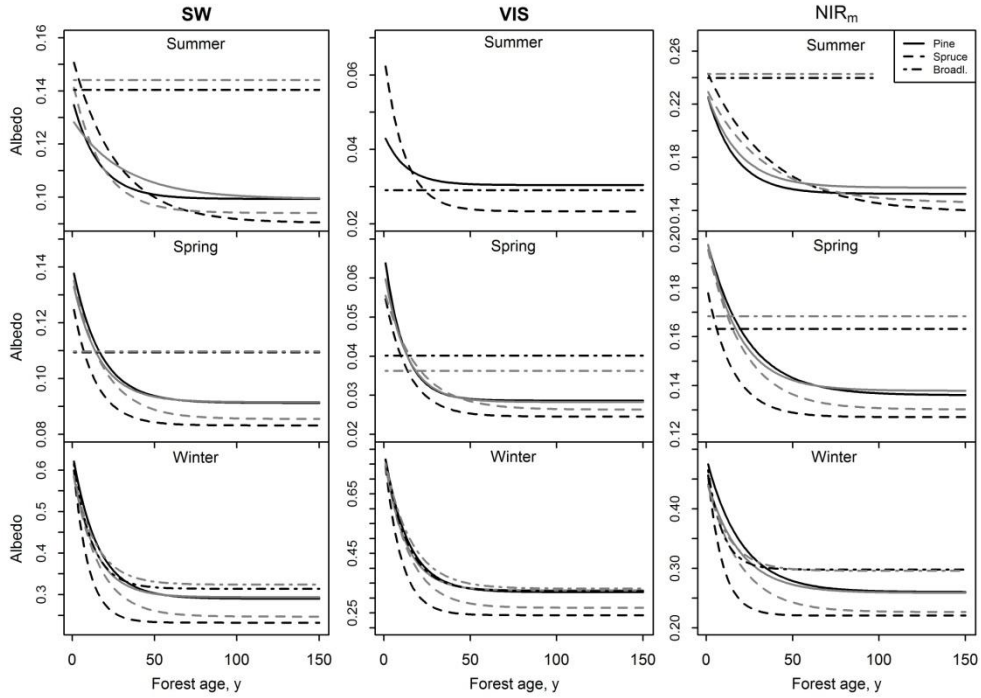

Figure 7. Albedo-age relationships estimated from MODIS albedo retrievals using linear unmixing for SW, VIS and NIR_m broadbands. During summer and spring, the broadleaved albedo represents the mean albedo of the species. Black and grey lines represent different albedo retrieval dates.

As already seen in the section 3.1 discussing albedo seasonality (studies I and III), the shortwave albedos were generally lowest in spring and highest in winter (Figure 7). NIR_m albedos followed the same pattern, but the VIS albedos for spruce and broadleaved species were lowest in summer. Visible albedos were higher than albedos in NIR_m in winter for all species, which should be due to the high albedo of snow in the visible spectral range (Wiscombe and Warren 1980). The decline rate of coniferous albedo was on average slightly higher for VIS than for NIR_m (Figure 7). A similar pattern of more rapid decrease of red band compared to NIR reflectance with stand age was also observed by Nilson and Peterson (1994) using airborne measurements. The pine albedos were already fairly stable at stands aged above ca. 50 years, but spruce NIR_m and SW albedos became saturated later than this in summer. The decrease in spruce NIR_m and SW albedos was more rapid in winter than summer. The age at which pine forest albedo became stable approximately coincides with the age when foliage biomass and canopy coverage in Scots pine forests are estimated to have reached their maxima (Mäkelä 1997), and agrees with the results of Nilson and Peterson (1994) and Rautianen et al. (2004). Rautiainen et al. (2004) found that simulated wavelength-specific directional reflectance factors decrease until a stand age of ca. 50 years in coniferous stands in Central Finland. The difference between the initial (seedling stand) and the saturated albedo value was higher for spruce than for pine in summer and winter, but similar in spring, while the saturated albedos of spruce were lower than those of pine or broadleaved species during all seasons. Pine forest albedo was lower

in winter than the albedo of broadleaved species in SW and NIR_m, but approximately equal in VIS. One reason for the fairly low broadleaved albedo in winter, particularly in VIS, could be the undergrowth of shade-tolerant spruces (Nilson and Peterson 1994). Moreover, no old broadleaved stands were included in the data, only broadleaved trees found as mixtures in the old conifer stands. It can also be thought that it was not the broadleaved albedo that was low in winter, but rather the pine albedo that was high. A high winter albedo of pine forests could result from high canopy snow interception, as discussed in section 3.1. Broadleaved deciduous species' albedo could not be estimated as an exponential function of age in summer or spring, which could be due to the following reasons. Firstly, it is possible that the albedo of broadleaved forests does not considerably vary with age in summer. For example, the in-situ-measured albedos of a seedling stand (although of spruce) and of a mature birch stand were similar. Secondly, the previously mentioned lack of old broadleaved stands in the study area might have made estimation impossible. It is thus not possible to draw any conclusions about the dependency of broadleaved forest albedo on forest age.

The difference in pine and spruce seedling stand albedos in summer is most likely due to differences in typical understorey vegetation in the seedling stands. Spruce is common on fertile soils, where the deciduous understorey vegetation and seedlings of broadleaved trees may be more abundant than on the generally poorer pine sites. This could increase the initial (seedling stand) albedo of spruce estimated from the MODIS data compared to that of pine. On the other hand, Landsat albedo data indicated that spruce albedo in NIR_m would actually be lower in very young stands and increase towards the age of ca. 10 years. The low initial NIR_m albedo might be caused by stronger soil preparation in the spruce sites after clearcutting compared to pine sites. As the green understorey and tree seedlings take over the disturbed vegetation and bare soil, the visible albedo decreases and the near-infrared albedo increases, until the increasing coniferous tree cover once again causes NIR_m albedo to decline. Concerning the considerable variation in factors such as possible seedling stand vegetation, development of the understorey vegetation with stand ageing, timing of the clearance of broadleaved trees etc., it is clear that the regression parameters obtained from the unmixing analysis are very rough averages. These reasons at least partly explain the rather high standard errors of the parameter estimates (shown in study IV) as well as the differences in species-specific parameter estimates within the seasons (the emergence of deciduous vegetation in spring and differences in winter snow cover between the aggregation periods also induce differences in the estimates). It was notable that the nonlinear regression estimation for summer VIS albedo was possible for only one of the two MODIS retrieval dates used in the analysis. The absolute differences in the VIS albedo of vegetated surfaces are small during the growing season, and thus even small errors in the data can cause problems in the parameter estimation. It is also possible that the decline of VIS albedo with increasing forest age is not exponential in shape, as indicated by the results of study V (section 3.2.3). The interpretation of the resultant parameter estimates is further complicated by the land cover pixels with unquantified growing stock (that is, species proportions could not be estimated) being assigned to the zero age class in the unmixing analysis. In practice, this means that stands with a tree height of less than 1.3 m and no reserve trees were classified as clear cuts and were not included in the albedo-age relationships.

3.2.3 Variation in understorey and canopy BRFs

Forest structure and understorey effects on Landsat nadir view BRFs were examined in study V. Both spruce and pine forest BRFs in the red, NIR and SWIR bands decreased when the measured or estimated forest variables of mean tree height, basal area, volume and LAI increased (Figure 8). The linear correlations between the forest variables and BRFs were much higher for spruce than for pine. A rapid decline would have occurred in BRFs during early succession had the young seedling stands been included in the analysis. The forest variables of both species were on average best correlated with the BRFs in SWIR; a result that agrees with the findings of previous studies (Brown et al. 2000; Stenberg et al. 2004; Heiskanen et al. 2011). Pine forest BRF in NIR showed a similar exponential decrease as a function of forest age as was noted in the satellite albedo data analysis, whereas no clear trend was observed in the red band. Spruce BRFs in all wavebands showed a rapid decrease with forest age, but at very high stand ages (> 170 years) the BRFs increased again; these old forests were also characterised by low canopy cover and volume.

Why did the pine forest BRFs correlate so poorly with the forest variables? One possible reason could be the on average higher fraction of the sunlit understorey and the possibly wider range in understorey optical properties due to a wider range in soil fertility and thus in understorey vegetation in pine compared to spruce forests. These two factors together might lead to poor correlation between pine forest BRFs and forest structural variables. However, the unmixing models that took into account the variation in understorey and canopy BRFs in three discrete site fertility and stand development classes did not explain a much higher degree of variation in the pine forest BRFs. It can thus be assumed that either large variation occurred in the component BRFs within the classes, or the component fractions were not properly estimated. Both reasons seem likely as, first of all, it is clear that the understorey vegetation composition varies within the ecologically broad fertility classes and within the geographical range of the field plots. Variation in the "canopy and shaded ground" component BRFs was also likely not sufficiently accounted for by only three classes. An attempt was made to divide the forest scene into three components that could better describe the reflectance characteristics of the forest, namely "sunlit understorey", "shaded understorey" and "canopy". This, however, led to a too high number of parameters (with high uncertainty) to be estimated and to unreliable results. Secondly, simplifying assumptions were made to calculate the gap fraction for the estimation of the component fractions (f_u and $1\text{-}f_u$): it was assumed that the radiation extinction coefficient was species-specific and that it did not change with zenith angle. The first assumption neglects the site-specific factors that may affect clumping; for instance, the possibly more highly clumped tree distribution in naturally regenerated or sown pine stands than in manually planted ones. The second assumption, in turn, is in conflict with the general observation that the apparent clumping decreases with increasing zenith angle (e.g. Kucharik et al. 1999). The canopy cover estimates in the inventory data additionally contain some error and the location errors between the Landsat pixels and field plots cause uncertainty to the forest variable estimates within the pixels.

BRFs of the "sunlit understorey" component estimated using nonlinear unmixing decreased as the forest matured and the site fertility decreased in NIR, but concurrently increased in red band and SWIR (Figure 9). The absolute changes were generally largest in the NIR spectral region. Reasons for the high understorey reflectance in NIR in the young

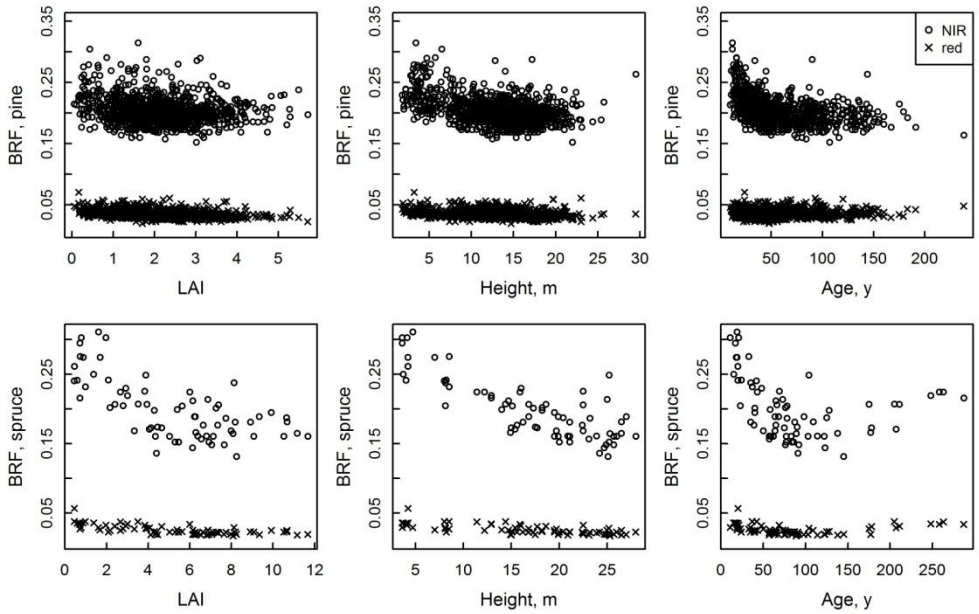

Figure 8. Pine and spruce BRFs in the Landsat NIR and red wavebands as a function of forest variables LAI, mean height, and forest age.

stands were already discussed in section 3.2.2, and should include the higher amount of grasses, herbs and deciduous tree seedlings in the young stands compared to the mature, closed-canopy coniferous forests, which are often dominated by mosses and dwarf shrubs (Hotanen et al. 2001). A similar explanation could be found for the higher NIR reflectance on mature fertile sites compared to infertile sites; the amount of grasses and herbs on fertile sites can remain comparatively higher throughout the succession (Hotanen et al. 2001). The understorey measurements conducted as part of the in-situ albedo measurements also indicated that sites with grass- and herb-dominated understories have higher shortwave albedos than moss- and dwarf shrub-dominated ones. The very poor *Calluna* -type (CT) forests had on average lower NIR and higher SWIR and red band BRFs than the other fertility classes. The high BRF in SWIR could be explained by the dry soil and sparse understorey vegetation, the latter also being a likely reason for the low BRF in the NIR and high in the red band. In fact the BRF in NIR of the "canopy and shaded ground" component was higher than that of the "sunlit understorey" in CT, unlike in the other fertility classes. Site P3 represented this fertility class, and it was indeed observed that the understorey shortwave albedo of this site was lower than the whole-stand albedo. However, this can be attributable to an unrepresentative understorey albedo measurement spot within the plot, where the ground cover was very heterogeneous.

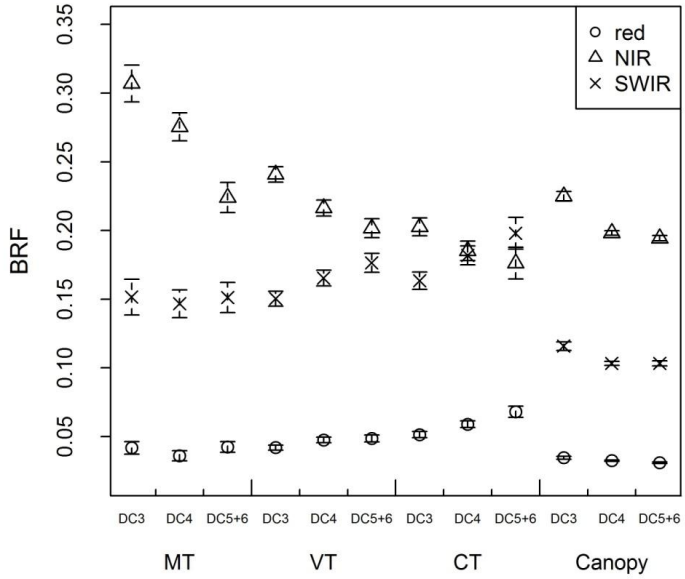

Figure 9. Pine forest BRFs ± standard error in red, NIR and SWIR at different site fertility and stand development classes.

The BRF of the "canopy and shaded ground" component somewhat decreased during stand development in the pine forests, particularly in NIR and when moving from the first development class (mature seedling stand) to the second one (young thinning stand) (Figure 9). Such a decrease could be caused by the increasing amount of total foliage biomass and changes in the proportions of sunlit and shaded crown areas during early succession (Nilson and Peterson 1994). BRF in NIR was best explained by mean tree height of both species, while the correlation between NIR BRF and canopy cover was clearly poorer than that between red or SWIR BRF and canopy cover. Because canopy cover was used to estimate the fractions of the components "sunlit understorey" and "canopy and shaded ground", the addition of mean height as an explanatory variable for the regression of spruce noticeably increased the coefficient of determination (R^2) in NIR, but less in red. Note that the canopy development class for spruce, unlike for pine, was not accounted for in the unmixing analysis of the component BRFs. Perhaps in red, where multiple scattering of radiation within the canopy and between the canopy and ground is smaller than in NIR, the BRF is better explained purely by the fractional covers of the understorey and canopy with different BRFs. It was furthermore observed that in spruce forests the fraction of sunlit understorey saturates before the BRF in NIR. In other words, canopy development caused a decrease in forest reflectance even after the influence of the sunlit understorey had reached its minimum.

Overall, the results of the unmixing analysis indicated that canopy development changes the influence of the understorey on forest BRF in two ways: increasing canopy cover obviously decreases the fraction of forest floor visible to the sensor, but additionally changes the understory vegetation composition so that the sunlit understorey BRFs vary during stand development. A more accurate estimation of the component BRFs, or BRFs of

the separated sunlit and shaded canopy and ground would require more detailed estimates of the component fractions and therefore detailed measurements of forest structure. The BRFs obtained in study V are not directly translatable into albedo units. Information on the bidirectional reflectance distribution function (BRDF) of the target surfaces would be needed to be able to estimate the spectral albedos, and on the spectral to broadband conversion factors to estimate the broadband albedos. However, the results give indication on how spectral albedos vary with forest variables or site fertility.

3.2.4 Spatial variation in forest albedo

The variation in forest albedo and reflectance both within and between tree species is driven by optical and structural forest characteristics. It seems that the differences in albedo between tree species outweigh the differences within species with differing canopy structure in middle aged and mature forests. The difference between spruce and birch albedos measured in-situ was approximately 0.09 and that between spruce and pine forests 0.03 during the growing season (study II). This difference between coniferous and broadleaved deciduous forest albedos was even higher in February with snow-covered ground, reaching up to 0.16 as estimated from MODIS albedo retrievals. The influence of the understorey and deciduous mixture is higher during early succession, and separating between pine and spruce stands may not be possible or meaningful. When the estimated albedo-age relationships were used to predict the MODIS test data set albedos in study IV, it was noted that predictions were only slightly more accurate than when only species-specific mean albedos were used. However, it was evident that the estimated albedo-age relationships did not cover all variation in species-specific albedos (section 3.3). Even though the high albedo phase in the beginning of a rotation is rather short (Figure 7), the influence of these forests on the landscape (MODIS pixel) -level albedo should be noticeable due to their relatively high share (1-20 year old forests account for ca. 20% of all forests in the area, Korhonen et al. 2013).

The result of study V, according to which spruce forest reflectance would be more sensitive to forest structural variables than the reflectance of pine forests, agreed with the finding made in study IV that albedo was saturated sooner in pine than in spruce forests with increasing forest age. This was on one hand attributed to the greater influence of the understorey on forest reflectance in pine compared to spruce forests, and on the other to the maximum amount of foliage biomass achieved at fairly young stand ages in pine forests. These results are in contradiction with the similar albedos of the dense and sparse spruce stands measured in study II. Forest albedo or BRF responses to structural forest variables, or to the variation in the proportions of forest elements with different optical properties with forest age, was dependent on wavelength. The results indicate that forest reflectance in the visible wavelength region could be more sensitive to canopy cover and understorey reflectance (study V) and saturate sooner with stand development than the reflectance in NIR (study IV), which in contrast had a stronger response to some structural forest variables, such as forest height (study V). Shortwave albedo could be more robust than spectral reflectance to variation in forest characteristics within tree species. For example, results of study V showed that as pine forest fertility decreased, the understorey BRF in NIR decreased, but on the other hand, the BRFs in red and SWIR increased, which should lead to a smaller effect of site fertility on forest shortwave albedo than on spectral BRFs or albedos.

3.3 Comparison of albedo retrieval methods

Compared to in-situ-measured pine, spruce and birch forest albedos, the summer albedos estimated from MODIS using linear unmixing in study III overestimated the lowest albedos (spruce albedo) and underestimated the albedo for the component with the highest measured albedo (birch). For pine, the albedo estimated using unmixing was close to the measured value. Only a few stands of each species were measured, and the comparison is thus only approximate. When component albedos produced by unmixing were compared to albedos of homogeneous pixels (for components for which homogeneous pixels existed), the two estimates were fairly close to each other.

Quality of the MODIS albedo retrievals used in this study was generally reported poor in midwinter. Error in the MODIS albedo is shown to increase as the SZA increases beyond the MODIS view angle range (Liu et al. 2009), and albedos estimated for SZAs greater than 70-75˚ are not recommended to be used. The winter MODIS albedos used in study IV were from DOY 41 with a noon SZA of ca. 76˚ in the study area. A proper comparison of the winter albedos estimated from MODIS 16-day albedo products against field observations could be difficult due to the constantly changing albedo of a snow covered forest. Xin et al. (2012) suggested that snow cover modelling using MODIS images acquired from off-nadir view angles can lead to underestimation of the snow cover fraction in forested regions. It might consequently be expected that the albedo of snow-covered forests could be underestimated compared to pyranometer measurements (Muller et al. 2013), at least unless the canopy is snow covered.

When the albedo-age relationships estimated from MODIS data by linear unmixing were used to predict albedos for the test data in study IV, the predicted values were close to the mean data set albedos. In other words, the slopes of the linear least squares regressions of the predicted against observed test data set albedos were rather low, and the range of the predicted albedos lower than that of the observed ones. Moreover, when the albedo-age relationships estimated from Landsat albedo data without unmixing were used to predict the MODIS test data set albedos, the slopes of the predicted vs. observed albedos were clearly higher than when relationships derived from MODIS were used. However, the absolute values of MODIS and Landsat blue-sky albedos in study IV were not directly comparable due to different years of acquisition (2010 and 2011, respectively), processing methods and illumination conditions. Landsat-derived albedos were also closer to the highest (birch) and lowest (spruce) forest albedos measured in field in study II than those estimated from MODIS data using unmixing. Compared to the in-situ-measured seedling stand (C) shortwave albedos, the ones estimated from both MODIS and Landsat were generally lower, although Landsat spruce forest albedos reached similar values at their maximum at about 15 years of age.

Errors in the predictor variables were likely high and thus the unmixing models did not explain all the variation around the mean data set albedos. Error was introduced at various stages to the predictor variables, stand age and species proportions estimated from growing stock. The pixel-level error of the variables produced by ik-NN can be rather high (Tomppo et al. 2008a). Further error is caused when these data are matched to the response variables, because the area of the predefined MODIS grid cells does not correspond to the true observation area when scanned from off-nadir view angles, i.e. the spatial resolution of the pixels on the edge of the swath is coarser than that in the centre (Wolfe et al. 1998; Lucht et al. 2000; Tan et al. 2006). In addition, correlations between the component fractions add uncertainty to the parameter estimates due to unstable matrix inversion. Results are also

dependent on the components selected for the unmixing; high variation in albedo within the components (i.e. in albedo within species in study III, and in albedo within species at certain forest age in study IV), would increase the uncertainty of the estimated parameters. For example, the effect of site fertility on growth rate, which might add variation to the albedo at a specific forest age, was not accounted for in the albedo-age relationships because the amount of unknown parameters would have become too high.

Uncertainty related to the predictor variables and to the spatial matching of the predictors and response variables, as well as the need to have preliminary information on albedo variation as a function of the predictor variables, makes it difficult to use linear unmixing to estimate complicated functions with many unknown parameters from the coarse spatial resolution satellite albedo retrievals. Considering MODIS albedos, this method could be useful when temporally frequent albedo estimates are needed of land cover types that clearly differ in their spectral properties. In addition, using coarser spatial resolution albedo data might reduce the spatial mismatch problem.

Forest albedo model PARAS was used to predict broadband albedos for the in-situ albedo measurement sites (study II). The shortwave albedos were fairly accurately predicted for the coniferous stands, but PAR albedos were clearly underestimated by the model (Fig. 6). On the other hand, the shortwave albedo for the birch stand was overestimated by the model, but PAR albedo was close to the measured one. Reasons that might cause discrepancy between the measured and modelled albedos include the possible error in the input parameters used in the modelling (LAI and foliage and understorey spectra), and also inaccuracy in the wavelength dependency of parameters p (the recollision probability) and Q (the fraction of backward scattering). More precisely, it has been suggested that the probability for an intercepted photon to escape the forest should be higher for the first canopy interactions (Mõttus and Stenberg 2008). Correcting for this would increase reflectance relatively more in the PAR than in the NIR wavelengths, because leaf albedos in PAR are low and first-order scattering dominates. A sensitivity analysis suggested that the strong overestimation of the birch stand shortwave albedo by the model could be due to too high leaf albedos in the NIR region. Additionally, weighting the foliage spectra by that of the branches, with lower albedo in NIR than the leaves, would have decreased the modelled birch albedo. Also, as already noted, the mast measurements are not free of error. Forest reflectance modelling was a useful tool in helping to understand the effects of changing forest parameters on forest albedo. For example, with increasing LAI, the recollision probability and thus absorptance increased, and albedo decreased. However, the fraction of backscattering (Q) concurrently increased, which made the decline in albedo slower.

The forest stands used in albedo measurements and modelling were ideal for a modelling exercise considering their relatively simple structure and species composition. In reality however, even managed forests often consist of more than one tree species or tree layer. Quantification of the effect of tree species mixture in both under- and overstorey on forest summer and winter albedo could therefore be an interesting subject for future research.

4 CONCLUSIONS

Understanding the patterns in forest and landscape shortwave albedo, as well as retrieving accurate estimates of them is important for the accurate description of the energy exchange between different land cover types and the atmosphere in weather and climate models, and perhaps also for future land use planning. The most accurate albedo estimates can naturally be obtained from in-situ measurements using pyranometers. However, is not possible to cover the large variation in landscape and forest structure and therefore in albedo using such measurements. Remote sensing and modelling approaches can thus often be more feasible options. In this thesis, these methods were used to examine variation in forest albedo due to temporally and spatially varying factors such as snow cover, species composition and forest age and structure.

The effect of snow cover on forest albedo was estimated using in-situ albedo measurements. The varying amount and optical properties of snow as well as changing illumination conditions led to high variation in pine forest albedo during the snow-cover period. Albedo typically increased as the amount of snow in the tree canopy increased.

The seasonal variation in forest and landscape albedo was estimated using in-situ albedo measurements as well as satellite albedo retrievals. Seasonal variation in landscape albedo was most pronounced in open land cover types, where the ground snow was not obscured by trees in winter. The broadleaved deciduous forests typically had a higher albedo than the coniferous forests during all seasons in southern Finland. The albedo of coniferous forests was fairly stable during the snow-free period.

Both the in-situ albedo measurements and the analysis of the satellite albedo retrievals indicated that a large part of the albedo variation of a forested landscape can be explained by tree species only. In young stands, however, the fraction of visible understorey and broadleaved deciduous tree seedlings can be high and the albedo is less dependent on the managed tree species and higher than in mature forests. Results of the effects of forest structure on forest albedo were slightly controversial between the studies using satellite-derived albedo data and in-situ pyranometer measurements, but the sample size of the in-situ albedo measurements was inevitably very small. Compared to in-situ measurements, satellite albedo data may be better for distinguishing patterns in albedo due to surface characteristics, such as forest structure, whereas the advantages of in-situ pyranometer measurements are the spatially explicit and temporally comprehensive albedo estimates.

Changes in LAI or canopy cover may have a negligible impact on shortwave albedo in forests with a relatively low understorey albedo, such as the dwarf shrub- and moss-dominated coniferous stands measured in-situ. Such forests are common in Finland, which might undermine the possibility of influencing albedo of managed forests during the snow-free season by intensifying thinning regimes. Based on the results presented here, the most obvious way in which forest albedo can be controlled by silvicultural options is thus the choice of tree species. The in-situ albedo measurements showed that mature spruce forests may have albedos that are approximately 0.03 and 0.09 units lower than those in pine and birch forests, respectively. The differences were even higher during the snow-cover period. Shortening the rotation period and thus increasing the relative length of the high albedo phase at the beginning of the rotation would obviously increase landscape albedo, but could have undesired effects on timber yield, carbon sequestration and biodiversity.

REFERENCES

Alekseyev V.A. & Birdsey R.A. (1998). Carbon storage in forests and peatland of Russia. Gen. Tech. Rep. NE-244. Radnor, PA: U.S. Department of Agriculture, Forest Service, Northeastern Forest Experiment Station. 137 p.

Anderson R.G., Canadell J.G., Randerson J.T., Jackson R.B., Hungate B.A., Baldocchi D.D. et al. (2010). Biophysical considerations in forestry for climate protection. Frontiers in Ecology and the Environment 9: 174-182. http://dx.doi.org/10.1890/090179

Amiro B.D., Orchansky A.L., Barr A.G., Black T.A., Chambers S.D., Chapin III F.S. et al. (2006). The effect of post-fire stand age on the boreal forest energy balance. Agricultural and Forest Meteorology 140: 41-50. http://dx.doi.org/10.1016/j.agrformet.2006.02.014

Arora V.K. & Montegenro A. (2011). Small temperature benefits provided by realistic afforestation efforts. Nature Geoscience 4: 514-518. http://dx.doi.org/10.1038/ngeo1182

Baker D.G., Ruschy D.L., Wall D.B. (1990). The albedo decay of prairie snows. Journal of Applied Meteorology 29: 179-187. http://dx.doi.org/10.1073/pnas.0608998104

Bala G., Caldeira K., Wickett M., Phillips T.J., Lobell D.B., Delire C., Mirin A. (2007). Combined climate and carbon-cycle effects of large-scale deforestation. Proceedings of the National Academy of Sciences of the United States of America 104: 6550-6555. http://dx.doi.org/10.1073/pnas.0608998104

Baldocchi D., Kelliher F.M., Black T.A., Jarvis P. (2000). Climate and vegetation controls on boreal zone energy exchange. Global Change Biology 6: 69-83. http://dx.doi.org/10.1046/j.1365-2486.2000.06014.x

Baldocchi D., Falge E., Gu L., Olson R., Hollinger D., Running S. et al. (2001). FLUXNET: A new tool to study the temporal and spatial variability of ecosystem-scale carbon dioxide, water vapor, and energy flux densities. Bulletin of the American Meteorological Society 82: 2415-2434. http://dx.doi.org/10.1175/1520-0477(2001)082<2415:FANTTS>2.3.CO;2

Bathiany S., Claussen M., Brovkin V., Raddatz T., Gayler V. (2010). Combined biogeophysical and biogeochemical effects of large-scale forest cover changes in the MPI earth system model. Biogeosciences 7: 1383-1399. http://dx.doi.org/10.5194/bg-7-1383-2010

Ben-Gai T., Bitan A., Manes A., Alpert P., Israeli A. (1998). Aircraft measurements of surface albedo in relation to climatic changes in Southern Israel. Theoretical and Applied climatology 61: 207-215. http://dx.doi.org/10.1007/s007040050065

Bernier P.Y., Desjardins R.L., Karimi-Zindashty Y., Worth D., Beaudoin A., Luo Y., Wang S. (2011). Boreal lichen woodlands: A possible negative feedback to climate change in eastern North America. Agricultural and Forest Meteorology 151: 521-528. http://dx.doi.org/10.1016/j.agrformet.2010.12.013

Betts A.K. & Ball J.H. (1997). Albedo over the boreal forest. Journal of Geophysical Research 102: 28901–28909. http://dx.doi.org/10.1029/96JD03876

Betts R.A. (2000). Offset of the potential carbon sink from boreal forestation by decreases

in surface albedo. Nature 408: 187-190.
http://dx.doi.org/10.1038/35041545

Betts R. (2007). Implications of land ecosystem-atmosphere interactions for strategies for climate change adaptation and mitigation. Tellus, Series B: Chemical and Physical Meteorology 59: 602-615.
http://dx.doi.org/10.1111/j.1600-0889.2007.00284.x

Betts A.K., Desjardins R.L., Worth D. (2007). Impact of agriculture, forest and cloud feedback on the surface energy budget in BOREAS. Agricultural and Forest Meteorology 142: 156-169.
http://dx.doi.org/10.1016/j.agrformet.2006.08.020

Bonan G.B., Pollard D., Thompson S.L. (1992). Effects of boreal forest vegetation on global climate. Nature 359: 716-718.
http://dx.doi.org/10.1038/359716a0

Bonan G.B., Chapin F.S. & Thompson S.L. (1995). Boreal forest and tundra ecosystems as components of the climate system. Climatic Change 29: 145-167.
http://dx.doi.org/10.1007/BF01094014

Bright R.M., Antón-Fernóndes C., Astrup R., Cherubini F., Kvalevåg M., Strømman A.H., Peters G.P. (2014). Climate change implications of shifting forest management strategy in a boreal forest ecosystem of Norway. Global Change Biology 20: 607-621. http://dx.doi.org/10.1111/gcb.12451

Brown L., Chen J.M., Leblanc S.G., Cihlar J. (2000). A shortwave infrared modification to the simple ratio for LAI retrieval in boreal forests: An image and model analysis. Remote Sensing of Environment 71: 16-25.
http://dx.doi.org/10.1016/S0034-4257(99)00035-8

Cajander A.K. (1949). Forest types and their significance. Acta Forestalia Fennica 56: 1-69.

Ceccato P., Flasse S., Tarantola S., Jacquemoud S., Grégoire J.-M. (2001). Detecting vegetation leaf water content using reflectance in the optical domain. Remote Sensing of Environment 77: 22-33.
http://dx.doi.org/10.1016/S0034-4257(01)00191-2

Cescatti A., Marcolla B., Santhana Vannan S.K., Pan J.Y., Román M.O., Yang X. et al. (2012). Intercomparison of MODIS albedo retrievals and in situ measurements across the global FLUXNET network. Remote Sensing of Environment 121: 323-334. http://dx.doi.org/10.1016/j.rse.2012.02.019

Chen J.M. & Cihlar J. (1996). Retrieving leaf area index of boreal conifer forests using Landsat TM images. Remote Sensing of Environment 55: 153-162.
http://dx.doi.org/10.1016/0034-4257(95)00195-6

Chen X. & Vierling L. (2006). Spectral mixture analyses of hyperspectral data acquired using a tethered balloon. Remote Sensing of Environment 103: 338-350. http://dx.doi.org/10.1016/j.rse.2005.05.023

Csiszar I. & Gutman G. (1999). Mapping global land surface albedo from NOAA AVHRR. Journal of Geophysical Research 104: 6215-6228.
http://dx.doi.org/10.1029/1998JD200090

Davidson A. & Wang S. (2004). The effects of sampling resolution on the surface albedos of dominant land cover types in the North American boreal region. Remote Sensing of Environment 93: 211-224.
http://dx.doi.org/10.1016/j.rse.2004.07.005

Davidson A. & Wang S. (2005). Spatiotemporal variations in land surface albedo across

Canada from MODIS observations. Canadian Journal of Remote Sensing 31: 377-390. http://dx.doi.org/10.5589/m05-021

Davin E.L., de Noblet-Ducoudré N., Friedlingstein P. (2007). Impact of land cover change on surface climate: Relevance of the radiative forcing concept. Geophysical Research Letters 34: L13702. http://dx.doi.org/10.1029/2007GL029678

Deering D.W., Eck T.F., Banerjee B. (1999). Characterization of the reflectance anisotropy of three Boreal forest canopies in spring-summer. Remote Sensing of Environment 67: 205-229. http://dx.doi.org/10.1016/S0034-4257(98)00087-X

Dickinson R.E. (1983). Land surface processes and climate - surface albedos and energy balance. Advances in Geophysics 25: 305-353.

Eriksson H.M., Eklundh L., Kuusk A., Nilson T. (2006). Impact of understory vegetation on forest canopy reflectance and remotely sensed LAI estimates. Remote Sensing of Environment 103: 408-418. http://dx.doi.org/10.1016/j.rse.2006.04.005

Eugster W., Rouse W.R., Pielke Sr. R.A., Mcfadden J.P., Baldocchi D.D., Kittel T.G.F. et al. (2000). Land-atmosphere energy exchange in Arctic tundra and boreal forest: Available data and feedbacks to climate. Global Change Biology 6: 84-115. http://dx.doi.org/10.1046/j.1365-2486.2000.06015.x

Federer C.A. (1968). Spatial variation of net radiation, albedo and surface temperature of forests. Journal of Applied Meteorology 7: 789-795. http://dx.doi.org/10.1175/1520-0450(1968)007<0789:SVONRA>2.0.CO;2

Ganguly S., Schull M.A., Samanta A., Shabanov N.V., Milesi C., Nemani R.R. et al. (2008). Generating vegetation leaf area index earth system data record from multiple sensors. Part 1: Theory. Remote Sensing of Environment 112: 4333-4343. http://dx.doi.org/10.1016/j.rse.2008.07.014

Gardner A.S. & Sharp M.J. (2010). A review of snow and ice albedo and the development of a new physically based broadband albedo parameterization. Journal of Geophysical Research 115: F01009. http://dx.doi.org/10.1029/2009JF001444

Gates D.M. (1980). Biophysical Ecology. Dover Publications, Mineola, New York, 611 p.

Gates D.M., Keegan H.J., Schleter J.C., Weidner V.R. (1965). Spectral properties of plants. Applied Optics 4: 11-20. http://dx.doi.org/10.1364/AO.4.000011

Geiger B., Carrer D., Franchistéguy L., Roujean J.-L., Meurey C. (2008). Land surface albedo derived on a daily basis from meteosat second generation observations. IEEE Transactions on Geoscience and Remote Sensing 46: 3841-3856. http://dx.doi.org/10.1109/TGRS.2008.2001798

Gemmel F. (1999). Estimating conifer forest cover with thematic mapper data using reflectance model inversion and two spectral indices in a site with variable background characteristics. Remote Sensing of Environment 69: 105-121. http://dx.doi.org/10.1016/S0034-4257(99)00004-8

Grace J. (2004). Understanding and managing the global carbon cycle. Journal of Ecology 92: 189-202. http://dx.doi.org/10.1111/j.0022-0477.2004.00874.x

Hedtröm N.R. & Pomeroy J.W. (1998). Measurements and modelling of the snow interception in the boreal forest. Hydrological Processes 12: 1611–1625.

http://dx.doi.org/10.1002/(SICI)1099-1085(199808/09)12:10/11<1611::AID-HYP684>3.0.CO;2-4

Heiskanen J., Rautiainen M., Korhonen L., Mõttus M., Stenberg P. (2011). Retrieval of boreal forest LAI using a forest reflectance model and empirical regressions. International Journal of Applied Earth Observation and Geoinformation 13: 595-606. http://dx.doi.org/10.1016/j.jag.2011.03.005

Heiskanen J., Rautiainen M., Stenberg P., Mõttus M., Vesanto V.-H., Korhonen L., Majasalmi T. (2012). Seasonal variation in MODIS LAI for a boreal forest area in Finland. Remote Sensing of Environment 126: 104-115. http://dx.doi.org/10.1016/j.rse.2012.08.001

Hollinger D.Y., Ollinger S.V., Richardson A.D., Meyers T.P., Dail D.B., Martin M.E. et al. (2010). Albedo estimates for land surface models and support for a new paradigm based on foliage nitrogen concentration. Global Change Biology 16: 696-710. http://dx.doi.org/10.1111/j.1365-2486.2009.02028.x

Hotanen J.-P., Korpela L., Mikkola K., et al. (2001) Metsä- ja suokasvien yleisyys ja runsaus 1951-95. In: Reinikainen A., Mäkipää R., Vanha-Majamaa I., Hotanen J.-P. (ed.) Kasvit muuttuvassa metsäluonnossa.. Gummerus Kirjapaino Oy, Jyväskylä. p. 84-301.

Jacovides C.P., Tymvios F.S., Assimakopoulos V.D., Kaltsounides N.A. (2007). The dependence of global and diffuse PAR radiation components on sky conditions at Athens, Greece. Agricultural and Forest Meteorology 143: 277-287. http://dx.doi.org/10.1016/j.agrformet.2007.01.004

Jin Y., Schaaf C.B., Gao F., Li X., Strahler A.H., Zeng X., Dickinson R.E. (2002). How does snow impact the albedo of vegetated land surfaces as analyzed with MODIS data? Geophysical Research Letters 29. http://dx.doi.org/10.1029/2001GL014132

Kirschbaum M.U.F., Whitehead D., Dean S.M., Beets P.N., Shepherd J.D., Ausseil A.-G.E. (2011). Implications of albedo changes following afforestation on the benefits of forests as carbon sinks. Biogeosciences 8: 3687-3696. http://dx.doi.org/10.5194/bg-8-3687-2011

Kleman J. (1987). Directional reflectance factor distributions for two forest canopies. Remote Sensing of Environment 23: 83-96. http://dx.doi.org/10.1016/0034-4257(87)90072-1

Knyazikhin Y., Schull M., Xu L., Myneni R., Samanta A. (2011). Canopy spectral invariants. Part 1: A new concept in remote sensing of vegetation. Journal of Quantitative Spectroscopy and Radiative Transfer 112: 727-735. http://dx.doi.org/10.1109/WHISPERS.2009.5289105

Kobayashi H., Suzuki R., Kobayashi S. (2007). Reflectance seasonality and its relation to the canopy leaf area index in an eastern Siberian larch forest: Multi-satellite data and radiative transfer analyses. Remote Sensing of Environment 106: 238-252. http://dx.doi.org/10.1016/j.rse.2006.08.011

Kondratyev K.Ya. (1969). Raditation in the atmosphere. Academic Press, New York and London. 912 p.

Korhonen K., Ihalainen A., Viiri H., Heikkinen J., Henttonen H., Hotanen J.-P. et al. (2013). Suomen metsät 2004–2008 ja niiden kehitys 1921–2008. Metsätieteen aikakauskirja 3/2013: 269-608.

Kuusipalo J. (1983). Distribution of vegetation on mesic forest sites in relation to some characteristics of tree stand and soil fertility. Silva Fennica 17: 403-418.

Kucharic C.J., Norman J.M., Gower S.T. (1999). Characterization of radiation regimes in nonrandom forest canopies: theory, measurements, and a simplified modeling approach. Tree Physiology 19: 695-706. http://dx.doi.org/10.1093/treephys/19.11.695

Lafleur P.M. & Rouse W.R. (1995). Energy partitioning at treeline forest and tundra sites and its sensitivity to climate change. Atmosphere - Ocean 33: 121-133. http://dx.doi.org/10.1080/07055900.1995.9649527

Lafleur P.M., Wurtele A.B., Duguay C.R. (1997). Spatial and temporal variations in surface albedo of a subarctic landscape using surface-based measurements and remote sensing. Arctic and Alpine Research 29: 261-269. http://dx.doi.org/10.2307/1552140

Lang M., Kuusk A., Nilson T., Lükk T., Pehk M., Alm G. (2001). Reflectance spectra of ground vegetation in sub-boreal forests. http://www.aai.ee/bgf/ger2600/. [Cited 2013].

Larsen J.A. (1980). The boreal ecosystem. Academic Press, New York. 500 p.

Liang S. (2001). Narrow to broadband conversion of land surface albedo. I. Algorithms. Remote Sensing of Environment 76: 213-238. http://dx.doi.org/10.1016/S0034-4257(00)00205-4

Liu J., Schaaf C., Strahler A., Jiao Z., Shuai Y., Zhang Q. et al. (2009). Validation of moderate resolution imaging spectroradiometer (MODIS) albedo retrieval algorithm: Dependence of albedo on solar zenith angle. Journal of Geophysical Research: Atmospheres 114: D01106. http://dx.doi.org/10.1029/2008JD009969

LI-COR. (1992). LAI-2000 Plant Canopy Analyzer, Instruction Manual. LI-COR, Inc, Lincoln, Nebraska.

Lucht W., Schaaf C.B., Strahler A.H. (2000). An algorithm for the retrieval of albedo from space using semi-empirical BRDF models. IEEE Transactions on Geoscience and Remote Sensing 38: 977-998. http://dx.doi.org/10.1109/36.841980

Lukeš P., Stenberg P., Rautiainen M., Mõttus M., Vanhatalo K. (2013a). Optical properties of leaves and needles for boreal tree species in Europe. Remote Sensing Letters 4: 667-676. http://dx.doi.org/10.1080/2150704X.2013.782112

Lukeš P., Stenberg P., Rautiainen M. (2013b). Relationship between forest density and albedo in the boreal zone. Ecological Modelling 261-262: 74-79. http://dx.doi.org/10.1016/j.ecolmodel.2013.04.009

Manninen T. & Stenberg P. (2009). Simulation of the effect of snow covered forest floor on the total forest albedo. Agricultural and Forest Meteorology 149: 303-319. http://dx.doi.org/10.1016/j.agrformet.2008.08.016

Masek J.G., Vermote E.F., Saleous N., Wolfe R., Hall F.G., Huemmrich F. et al. (2006). A land surface reflectance data set for North America, 1990–2000. IEEE Geoscience and Remote Sensing Letters 3: 68-72. http://dx.doi.org/10.1109/LGRS.2005.857030

McCaughey J.H. (1981). Impact of clearcutting of coniferous forest on the surface radiation balance. Journal of Applied Ecology 18: 815-826. http://dx.doi.org/10.2307/2402372

McRoberts R.E. & Tomppo E.O. (2007). Remote sensing support for national forest inventories. Remote Sensing of Environment 110: 412-419. http://dx.doi.org/10.1016/j.rse.2006.09.034

Melloh R.A., Hardy J.P., Davis R.E., Robinson P.B. (2001). Spectral albedo/reflectance of

littered forest snow during the melt season. Hydrological Processes 15: 3409-3422. http://dx.doi.org/10.1002/hyp.1043

©Metsähallitus. (2012). Data owned by the Finnish State Forest Enterprise (Metsähallitus).

Miller J.R., White H.P., Chen J.M., Peddle D.R., McDermid G., Fournier R.A. et al. (1997). Seasonal change in understory reflectance of boreal forests and influence on canopy vegetation indices. Journal of Geophysical Research: Atmospheres 102: 29475-29482. http://dx.doi.org/10.1029/97JD02558

Monteith J.L. (1959). The reflection of short-wave radiation by vegetation. Quarterly Journal of the Royal Meteorological Society 86: 579. http://dx.doi.org/10.1002/qj.49708536607

Moody E.G., King M., Schaaf C.B., Hall D.K., Platnick S. (2007). Northern Hemisphere five-year (2000-2004) spectral albedos of surface in the presence of snow: Statistics computed from Terra MODIS land products. Remote Sensing of Environment 111: 337-345. http://dx.doi.org/10.1016/j.rse.2007.03.026

Moore C.J. (1976). A comparative study of radiation balance above forest and grassland. Quarterly Journal of the Royal Meteorological Society 102: 889-899. http://dx.doi.org/10.1002/qj.49710243416

Mõttus M. & Stenberg P. (2008). A simple parameterization of canopy reflectance using photon recollision probability. Remote Sensing of Environment 112: 1545-1551. http://dx.doi.org/10.1016/j.rse.2007.08.002

Mõttus M., Sulev M., Baret F., Lopez R., Reinart A. (2012). Photosynthetically active radiation: measurement and modeling. In: Encyclopedia of Sustainability Science and Technology. Meyers, R. (ed.). Springer, p. 7970-8000.

Muller J.-P., López G., Watson G., Shane N., Kennedy T., Yuen P. et al. (2012). The ESA GlobAlbedo Project for mapping the Earth's land surface albedo for 15 Years from European Sensors. IEEE Geoscience and Remote Sensing Symposium (IGARSS) 2012, IEEE, Munich, Germany, 22-27.7.12.

Muller J.-P. et al. (2013). GlobAlbedo final validation report. http://www.globalbedo.org/docs/GlobAlbedo_FVR_V1_2_web.pdf. [Cited 2014].

Mäkelä A. (1997). A carbon balance model of growth and self-pruning in trees based on structural relationships. Forest Science 43: 7-24.

Ni W. & Woodcock C.E. (2000). Effect of canopy structure and the presence of snow on the albedo of boreal conifer forests. Journal of Geophysical Research: Atmospheres 105: 11879-11888. http://dx.doi.org/10.1029/1999JD901158

Nilson T. & Peterson U. (1994). Age dependence of forest reflectance: analysis of main driving factors. Remote Sensing of Environment 48: 319-331. http://dx.doi.org/10.1016/0034-4257(94)90006-X

Nilson T. (1999). Inversion of gap frequency data in forest stands. Agricultural and Forest Meteorology 98-99: 437-448. http://dx.doi.org/10.1016/S0168-1923(99)00114-8

Nilson T., Olsson H., Anniste J., Lükk T., Praks J. (2001). Thinning-caused change in reflectance of ground vegetation in boreal forest. International Journal of Remote Sensing 22: 2763-2776. http://dx.doi.org/10.1080/01431160120213

Nilson T., Kuusk A., Lang M., Lükk T. (2003). Forest reflectance modeling: theoretical aspects and applications. Ambio 32: 535-541.

Nilson T., Suviste S., Lükk T., Eenmäe A. (2008). Seasonal reflectance course of some

forest types in Estonia from a series of Landsat TM and SPOT images and via simulation. International Journal of Remote Sensing 29: 5073-5091. http://dx.doi.org/10.1080/01431160802167543

Norman J.M. & Jarvis P.G. (1974). Photosynthesis in Sitka spruce (*Picea sitchensis* (Bong.) Carr.). III. Measurements of canopy structure and interception of radiation. Journal of Applied Ecology 11: 375-398. http://dx.doi.org/10.2307/2402028

Norman J.M. & Jarvis P.G. (1975). Photosynthesis in Sitka spruce (*Picea sitchensis* (Bong.) Carr.). V. Radiation penetration theory and a test case. Journal of Applied Ecology 12: 839-878. http://dx.doi.org/10.2307/2402094

Oker-Blom P. & Kellomäki S. (1983). Effect of grouping of foliage on the within-stand and within-crown light regime: comparison of random and grouping canopy models. Agricultural Meteorology 28: 143-155. http://dx.doi.org/10.1016/0002-1571(83)90004-3

Olsson H. (1994). Changes in satellite-measured reflectances caused by thinnig cuttings in boreal forests. Remote Sensing of Environment 50: 221-230. http://dx.doi.org/10.1016/0034-4257(94)90072-8

ORNL DAAC. (2012). https://daac.ornl.gov/cgi-bin/MODIS/GLBVIZ_1_Glb/ modis_ subset_order_global_col5.pl. [Cited 2012 and 2013].

Otterman J., Chou M.-D., Arking A. (1984). Effects of nontropical forest cover on climate. Journal of Applied Climatology and Meteorology 23: 762-767. http://dx.doi.org/10.1175/1520-0450(1984)023<0762:EONFCO>2.0.CO;2

Palmroth S. & Hari P. (2001). Evaluation of the importance of acclimation of needle structure, photosynthesis, and respiration to available photosynthetically active radiation in a Scots pine canopy. Canadian Journal of Forest Research 31: 1235-1243. http://dx.doi.org/10.1139/x01-051

Peltoniemi J.I., Kaasalainen S., Näränen J., Matikainen L., Piironen J. (2005). Measurement of directional and spectral signatures of light reflectance by snow. IEEE Transactions on Geoscience and Remote Sensing 43: 2294-2304. http://dx.doi.org/10.1109/TGRS.2005.855131

Pielke R.A. & Vidale P.L. (1995). The boreal forest and the polar front. Journal of Geophysical Research 100: 25755-25758. http://dx.doi.org/10.1029/95JD02418

Pinty B., Roveda F., Verstaete M.M., Gobron N., Govaerst Y., Martonchik J.V. et al. (2000). Surface albedo retrieval from Meteosat, 1. Theory. Journal of Geophysical Research 105: 18099-18112. http://dx.doi.org/10.1029/2000JD900113

Pomeroy J.W. & Dion K. (1996). Winter radiation extinction and reflection in a boreal pine canopy: Measurements and modelling. Hydrological Processes 10: 1591-1608. http://dx.doi.org/10.1002/(SICI)1099-1085(199612)10:12<1591::AID-HYP503>3.0.CO;2-8

Pomeroy J.W., Parviainen J., Hedstrom N., Gray D.M. (1998). Coupled modelling of forest snow interception and sublimation. Hydrological Processes 12: 2317-2337. http://dx.doi.org/10.1002/(SICI)1099-1085(199812)12:15<2317::AID-HYP799>3.0.CO;2-X

Qu X. & Hall A. (2007). What controls the strength of snow-albedo feedback? Journal of Climate 20: 3971-3981.

http://dx.doi.org/10.1175/JCLI4186.1
Ranson K.J., Irons J.R., Daughtry C.S.T. (1991). Surface albedo from bidirectional reflectance. Remote Sensing of Environment 35: 201-211. http://dx.doi.org/10.1016/0034-4257(91)90012-U
Ranson K.J., Irons J.R., Williams D.L. (1994). Multispectral bidirectional reflectance of northern forest canopies with the Advanced Solid-State Array Spectroradiometer (ASAS). Remote Sensing of Environment 47: 276-289. http://dx.doi.org/10.1016/0034-4257(94)90161-9
Rautiainen M., Stenberg P., Nilson T., Kuusk A. (2004). The effect of crown shape on the reflectance of coniferous stands. Remote Sensing of Environment 89: 41-52. http://dx.doi.org/10.1016/j.rse.2003.10.001
Rautiainen M. & Stenberg P. (2005). Application of photon recollision probability in coniferous canopy reflectance simulations. Remote Sensing of Environment 96: 98-107. http://dx.doi.org/10.1016/j.rse.2005.02.009
Rautiainen M., Mõttus M., Heiskanen J., Akujärvi A., Majasalmi T., Stenberg P. (2011). Seasonal reflectance dynamics of common understory types in a northern European boreal forest. Remote Sensing of Environment 115: 3020-3028. http://dx.doi.org/10.1016/j.rse.2011.06.005
Repola J. (2009). Biomass equations for Scots pine and Norway spruce in Finland. Silva Fennica 43: 605-624. http://dx.doi.org/10.14214/sf.184
Riihelä A. & Manninen T. (2008). Measuring the vertical albedo profile of a subarctic boreal forest canopy. Silva Fennica 42: 807-815.
Rock B.N., Williams D.L., Moss D.M., Lauten G.N., Kim M. (1994). High-spectral resolution field and laboratory optical reflectance measurements of red spruce and eastern hemlock needles and branches. Remote Sensing of Environment 47: 176-189. http://dx.doi.org/10.1016/0034-4257(94)90154-6
Roberts D.A., Ustin S.L., Ogunjemiyo S., Greenberg J., Bobrowski S.Z., Chen J., Hinckley T.M. (2004). Spectral and structural measures of northwest forest vegetation at leaf to landscape scales. Ecosystems 7: 545-562.
Román M.O., Schaaf C.B., Lewis P., Gao F., Anderson G.P., Privette J.L. et al. (2010). Assessing the coupling between surface albedo derived from MODIS and the fraction of diffuse skylight over spatially-characterized landscapes. Remote Sensing of Environment 114: 738-760. http://dx.doi.org/10.1016/j.rse.2009.11.014
Román M.O., Gatebe C.K., Shuai Y., Wang Z., Gao F., Masek J.G. et al. (2013). Use of in situ and airborne multiangle data to assess MODIS- and Landsat-based estimates of directional reflectance and surface albedo. IEEE Transactions on Geoscience and Remote Sensing 51: 1393-1403. http://dx.doi.org/10.1109/TGRS.2013.2243457
Ross J. (1981). The Radiation Regime and Architecture of Plant Stands. Dr. W. Junk Publishers, The Hague, 391 p.
Rouse W.R. (1984). Microclimate at arctic tree line 1. Radiation balance of tundra and forest. Water Resources Research 20: 57-66. http://dx.doi.org/10.1029/WR020i001p00057
Schaaf C.B., Gao F., Strahler A.H., Lucht W., Li X., Tsang T. et al. (2002). First operational BRDF, albedo nadir reflectance products from MODIS. Remote Sensing of Environment 83: 135-148.

http://dx.doi.org/10.1016/S0034-4257(02)00091-3
Schaepman-Strub G., Schaepman M.E., Painter T.H., Dangel S., Martonchik J.V. (2006). Reflectance quantities in optical remote sensing-definitions and case studies. Remote Sensing of Environment 103: 27-42. http://dx.doi.org/10.1016/j.rse.2006.03.002
Schleppi P., Conedera M., Sedivy I., Thimonier A. (2007). Correcting non-linearity and slope effects in the estimation of the leaf area index of forests from hemispherical photographs. Agricultural and Forest Meteorology 144: 236-242. http://dx.doi.org/10.1016/j.agrformet.2007.02.004
Sellers P.J., Meeson B.W., Hall F.G., Asrar G., Murphy R.E., Schiffer R.A. et al. (1995). Remote sensing of the land surface for studies of global change: models-algorithms-experiments. Remote Sensing of Environment 51: 3-26. http://dx.doi.org/10.1016/0034-4257(94)00061-Q
Settle J.J. & Drake N.A. (1993). Linear mixing and estimation of ground cover proportions. International Journal of Remote Sensing 14: 1159-1177. http://dx.doi.org/10.1080/01431169308904402
Sharratt B. S. (1998). Radiative exchange, near-surface temperature and soil water of forest and cropland in interior Alaska. Agricultural and Forest Meteorology 89: 269-280. http://dx.doi.org/10.1016/S0168-1923(97)00071-3
Shuai Y., Masek J.G., Gao F., Schaaf C.B. (2011). An algorithm for the retrieval of 30-m snow-free albedo from Landsat surface reflectance and MODIS BRDF. Remote Sensing of Environment 115: 2204-2216. http://dx.doi.org/10.1016/j.rse.2011.04.019
Sims D.A. & Gamon J.A. (2002). Relationships between leaf pigment content and spectral reflectance across a wide range of species, leaf structures and developmental stages. Remote Sensing of Environment 81: 337-354. http://dx.doi.org/10.1016/S0034-4257(02)00010-X
Smolander H., Stenberg P., Linder S. (1994). Dependence of light interception efficiency on structural parameters. Tree Physiology 14: 971-980. http://dx.doi.org/10.1093/treephys/14.7-8-9.971
Smolander S. & Stenberg P. (2003). A method to account for shoot scale clumping in coniferous canopy reflectance models. Remote Sensing of Environment 88: 363-373. http://dx.doi.org/10.1016/j.rse.2003.06.003
Smolander S. & Stenberg P. (2005). Simple parameterizations of the radiation budget of uniform broadleaved and coniferous canopies. Remote Sensing of Environment 94: 355-363. http://dx.doi.org/10.1016/j.rse.2004.10.010
Somers B., Cools K., Delalieux S., Stuckens J., Van der Zande D., Verstraeten W.W., Coppin P. (2009). Nonlinear Hyperspectral Mixture Analysis for tree cover estimates in orchards. Remote Sensing of Environment 113: 1183-1193. http://dx.doi.org/10.1016/j.rse.2009.02.003
Somers B., Asner G.P., Tits L., Coppin P. (2011). Endmember variability in Spectral Mixture Analysis: A review. Remote Sensing of Environment 115: 1603-1616. http://dx.doi.org/10.1016/j.rse.2011.03.003
Spracklen D.V., Bonn B., Carslaw K.S. (2008). Boreal forests, aerosols and the impacts on clouds and climate. Philosophical Transactions of the Royal Society A: Mathematical, Physical and Engineering Sciences 366: 4613-4626. http://dx.doi.org/10.1098/rsta.2008.0201
Stähli, M., Jonas, T., Gustafsson, D. (2009). The role of snow interception in winter-time

radiation processes of a coniferous sub-alpine forest. Hydrological Processes 23: 2498-2512. http://dx.doi.org/10.1002/hyp.7180

Stenberg P., Linder S., Smolander H. (1995). Variation in the ratio of shoot silhouette area to needle area in fertilized and unfertilized Norway spruce trees. Tree Physiology 15: 705-712. http://dx.doi.org/10.1093/treephys/15.11.705

Stenberg P., Kangas T., Smolander H., Linder S. (1999). Shoot structure, canopy openness, and light interception in Norway spruce. Plant, Cell, and Environment 22: 1133-1142. http://dx.doi.org/10.1046/j.1365-3040.1999.00484.x

Stenberg P., Rautiainen M., Manninen T., Voipio P., Smolander H. (2004). Reduced simple ratio better than NDVI for estimating LAI in Finnish pine and spruce stands. Silva Fennica 38: 3-14.

Stewart J.B. (1971). The albedo of a pine forest. Quarterly Journal of the Royal Meteorological Society 97: 561-564. http://dx.doi.org/10.1002/qj.49709741417

Strahler A.H. (1994). Vegetation canopy reflectance modelling – recent developments and remote sensing perspectives. Remote Sensing Reviews 15: 179-194. http://dx.doi.org/10.1080/02757259709532337

Stroeve J., Box J.E., Gao F., Liang S., Nolin A., Schaaf C. (2005). Accuracy assessment of the MODIS 16-day albedo product for snow: Comparisons with Greenland in situ measurements. Remote Sensing of Environment 94: 46-60. http://dx.doi.org/10.1016/j.rse.2004.09.001

Strugnell N.C., Lucht W., Schaaf C. (2001). A global albedo data set derived from AVHRR data for use in climate simulations. Geophysical Research Letters 28: 191-194. http://dx.doi.org/10.1029/2000GL011580

Tajchman S.J. (1972). The radiation and energy balances of coniferous and deciduous forests. Journal of Applied Ecology 9: 359-375. http://dx.doi.org/10.2307/2402437

Taillandier A.-S., Domine F., Simpson W.R., Sturm M., Douglas T.A. (2007). Rate of decrease of the specific surface area of dry snow: Isothermal and temperature gradient conditions. Journal of Geophysical Research: Earth Surface 112: F03003. http://dx.doi.org/10.1029/2006JF000514

Tan B., Woodcock C.E., Hu J., Zhang P., Ozdogan M., Huang D. et al. (2006). The impact of gridding artifacts on the local spatial properties of MODIS data: Implications for validation, compositing, and band-to-band registration across resolutions. Remote Sensing of Environment 105: 98-114. http://dx.doi.org/10.1016/j.rse.2006.06.008

Teuling A.J., Seneviratne S.I., Stöckli R., Reichstein M., Moors E., Ciais P. et al. (2010). Contrasting response of European forest and grassland energy exchange to heatwaves. Nature Geoscience 3: 722-727. http://dx.doi.org/10.1038/ngeo950

Thomas G. & Rowntree P.R. (1992). The boreal forests and climate. Quarterly Journal of the Royal Meteorological Society 118: 469-497. http://dx.doi.org/10.1002/qj.49711850505

Thompson M.P., Adams D., Sessions J. (2009). Radiative forcing and the optimal rotation age. Ecological Economics 68: 2713-2720. http://dx.doi.org/10.1016/j.ecolecon.2009.05.009

Thuillier G., Hersé M., Labs D., Foujols T., Peetermans W., Gillotay D. et al. (2003). The

solar spectral irradiance from 200 to 2400 nm as measured by the SOLSPEC spectrometer from the ATLAS and EURECA missions. Solar Physics 214: 1-22. http://dx.doi.org/10.1023/A:1024048429145

Tomppo E., & Halme M. (2004). Using coarse scale forest variables as ancillary information and weighting of variables in k-NN estimation: a genetic algorithm approach. Remote Sensing of Environment 92: 1-20. http://dx.doi.org/10.1016/j.rse.2004.04.003

Tomppo E., Olsson H., Ståhl G., Nilsson M., Hagner O., Katila M. (2008a). Combining national forest inventory plots and remote sensing data for forest databases. Remote Sensing of Environment 112: 1982-1999. http://dx.doi.org/10.1016/j.rse.2007.03.032

Tomppo E., Haakana M., Katila M., Peräsaari J. (2008b). Multi-source national forest inventory – Methods and applications. Managing Forest Ecosystems, vol. 18. Springer, Dortrecht, 374 p. ISBN 978-1-4020-8712-7.

Wang S. (2005). Dynamics of surface albedo of a boreal forest and its simulation. Ecological Modelling 183: 477-494. http://dx.doi.org/10.1016/j.ecolmodel.2004.10.001

Wang Z. & Zeng X. (2010). Evaluation of snow albedo in land models for weather and climate studies. Journal of Applied Meteorology and Climatology 49: 363-380. http://dx.doi.org/10.1175/2009JAMC2134.1

Wang Z., Schaaf C.B., Chopping M.J., Strahler A.H., Wang J., Román M.O. et al. (2012). Evaluation of Moderate-resolution Imaging Spectroradiometer (MODIS) snow albedo product (MCD43A) over tundra. Remote Sensing of Environment 117: 264-280. http://dx.doi.org/10.1016/j.rse.2011.10.002

Wang Z., Schaaf C.B., Strahler A.H., Chopping M.J., Román M.O, Shuai Y. et al. (2014). Evaluation of MODIS albedo product (MCD43A) over grassland, agriculture and forest surface types during dormant and snow-covered periods. Remote Sensing of Environment 140: 60-77. http://dx.doi.org/10.1016/j.rse.2013.08.025

Wanner W., Li X., Strahler A.H. (1995). On the derivation of kernels for kernel-driven models of bidirectional reflectance. Journal of Geophysical Research 100: 21077-21089. http://dx.doi.org/10.1029/95JD02371

Williams D.L. (1991). A comparison of spectral reflectance properties at the needle, branch, and canopy level for selected conifer canopies. Remote Sensing of Environment 35: 79-93. http://dx.doi.org/10.1016/0034-4257(91)90002-N

Wiscombe W.J. & Warren S.G. (1980). A model for the spectral albedo of snow. I: Pure snow. Journal of Atmospheric Sciences 37: 2712-2733. http://dx.doi.org/10.1175/1520-0469(1980)037<2712:AMFTSA>2.0.CO;2

Wolfe R.E., Roy D.P., Vermote E. (1998). MODIS land data storage, gridding, and compositing methodology: Level 2 grid. IEEE Transactions on Geoscience and Remote Sensing 36: 1324-1338. http://dx.doi.org/10.1109/36.701082

Xin Q., Woodcock C.E., Liu J., Tan B., Melloh R.A., Davis R.E. (2012). View angle effects on MODIS snow mapping in forests. Remote Sensing of Environment 118: 50-59. http://dx.doi.org/10.1016/j.rse.2011.10.029

Ångström A. (1925). The albedo of various surfaces of ground. Geografiska Annaler 7: 323-342. http://dx.doi.org/10.2307/519495